NASA CONTRACTOR REPORT

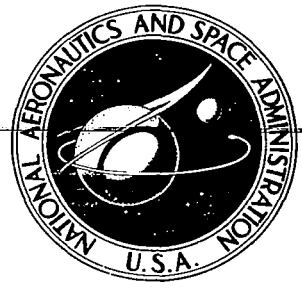

NASA-CR-2876

VIBROACOUSTIC RESPONSE OF STRUCTURES AND PERTURBATION REYNOLDS STRESS NEAR STRUCTURE-TURBULENCE INTERFACE

S. Maekawa and Y. K. Lin

Prepared by
UNIVERSITY OF ILLINOIS
Urbana-Champaign, Ill.
for Langley Research Center

NATIONAL AERONAUTICS AND SPACE ADMINISTRATION • WASHINGTON, D. C. • SEPTEMBER 1977

1. Report No.	2. Government Accession No.	3. Recipient's Catalog No.
NASA CR-2876		

4. Title and Subtitle	5. Report Date
Vibroacoustic Response of Structures and Perturbation Reynolds Stress Near Structure-Turbulence Interface	September 1977
	6. Performing Organization Code

7. Author(s)	8. Performing Organization Report No.
S. Maekawa and Y. K. Lin	
	10. Work Unit No. 505-03-11-02

9. Performing Organization Name and Address	11. Contract or Grant No.
University of Illinois Urbana-Champaign, IL	NSG-1264
	13. Type of Report and Period Covered
12. Sponsoring Agency Name and Address	Contractor Report
National Aeronautics & Space Administration Washington, DC 20546	14. Sponsoring Agency Code

15. Supplementary Notes

Langley technical monitor: Lucio Maestrello Final Report

16. Abstract This investigation is concerned with the interaction between a turbulent flow and certain types of structure responsing to its excitation. The turbulence is typical of those associated with a boundary layer, having a cross-spectral density indicative of convection and statistical decay. A number of structural models are considered in the investigation. Among the one-dimensional models are an unsupported infinite beam and a periodically supported infinite beam. The first model is used to develop the basic ideas which are then applied to the more realistic second model resembling the fuselage construction of an aircraft. For the two-dimensional case a simple membrane is used to illustrate the type of formulation applicable to most two-dimensional structures. However, a small random variation in the membrane tension is included in the analysis since ideally uniform tension never exists in practice. Moreover, the mathematical approach used in dealing with random membrane tension can be adapted to treat other random structural properties in general. Both the one-dimensional and two-dimensional structures mentioned above are backed by a cavity filled with an initially quiescent fluid to simulate the acoustic environment when the structure forms one side of a cabin of a sea- or air-craft.

It is shown that a decaying turbulence can be constructed from superposing infinitely many components, each of which is convected as a frozen-pattern at a different velocity. This superposition scheme reduces greatly the computation time by reducing to one-halp the number of integration which must be performed on a computer. Furthermore, the scheme provides a convenient way in which experimentally measured cross-spectral density of the turbulence pressure fluctuation can be incorporated directly in the computation.

The results of the structure-turbulence interaction are presented in terms of the spectral densities of the structural response and the perturbation Reynolds stress in the fluid at the vicinity of the interface. It is found that important spectral peaks of the structural response will not appear if decays in the turbulence are neglected in the analysis. Thus, the usual Taylor's hypothesis of frozen-pattern turbulence is unconservative as far as the assessment of structural reliability is concerned. The perturbation Reynolds stress is indicative of the change in the skin-friction drag due to structural motion. It is shown that, given the statistical information of the boundary-layer turbulent pressure field, the perturbation Reynolds stress can be changed by varying the structural parameters. Therefore, the presnet study if potentially useful for designing flight or marine structures to minimize the total skin-friction drag.

17. Key Words (Suggested by Author(s))	18. Distribution Statement
Panel Response Noise Radiated Boundary Layer Pressure Fluctuation	Unclassified - Unlimited Subject Category 39

19. Security Classif. (of this report)	20. Security Classif. (of this page)	21. No. of Pages	22. Price*
Unclassified	Unclassified	116	$5.50

*For sale by the National Technical Information Service, Springfield, Virginia 22161

FOREWORD

The report is based essentially on a Ph.D. thesis prepared by Shoji Maekawa under the supervision of Y. K. Lin. The research grant is administered by the Acoustics and Noise Reduction Division, NASA at Langley Research Center.

SUMMARY

This investigation is concerned with the interaction between a turbulent flow and certain types of structure responding to its excitation. The turbulence is typical of those associated with a boundary layer, having a cross-spectral density indicative of convection and statistical decay. A number of structural models are considered in the investigation. Among the one-dimensional models are an unsupported infinite beam and a periodically supported infinite beam. The first model is used to develope the basic ideas which are then applied to the more realistic second model resembling the fuselage construction of an aircraft. For the two-dimensional case a simple membrane is used to illustrate the type of formulation applicable to most two-dimensional structures. However, a small random variation in the membrane tension is included in the analysis since ideally uniform tension never exists in practice. Moreover, the mathematical approach used in dealing with random membrane tension can be adapted to treat other random structural properties in general. Both the one-dimensional and two-dimensional structures mentioned above are backed by a cavity filled with an initially quiescent fluid to simulate the acoustic environment when the structure forms one side of a cabin of a sea- or air-craft.

It is shown that a decaying turbulence can be con-

structed from superposing infinitely many components, each of which is convected as a frozen-pattern at a different velocity. This superposition scheme reduces greatly the computation time by reducing to one-half the number of integration which must be performed on a computer. Furthermore, the scheme provides a convenient way in which experimentally measured cross-spectral density of the turbulence pressure fluctuation can be incorporated directly in the computation.

The results of the structure-turbulence interaction are presented in terms of the spectral densities of the structural response and the perturbation Reynolds stress in the fluid at the vicinity of the interface. It is found that important spectral peaks of the structural response will not appear if decays in the turbulence is neglected in the analysis. Thus, the usual Taylor's hypothesis of frozen-pattern turbulence is unconservative as far as the assessment of structural reliability is concerned. The perturbation Reynolds stress is indicative of the change in the skin-friction drag due to structural motion. It is shown that, given the statistical information of the boundary-layer turbulent pressure field, the perturbation Reynolds stress can be changed by varying the structural parameters. Therefore, the present study is potentially useful for designing flight or marine structures to minimize the total skin-friction drag.

TABLE OF CONTENTS

Chapter		Page
I.	INTRODUCTION	1
II.	SPECTRAL ANALYSIS	
	2.1 Introduction	4
	2.2 The Statistical Properties of the Excitation	5
	2.3 Point-Load Analysis	8
	2.4 Frozen-Pattern Analysis	8
	2.5 Turbulence Decomposition Scheme - One-Dimensional Case	13
	2.6 Turbulence Decomposition Scheme - Two-Dimensional Case	16
	2.7 Conclusion	21
III.	UNSUPPORTED INFINITE BEAM	
	3.1 Introduction	23
	3.2 Wave-Number Response Function of the Infinite Unsupported Beam	23
	3.3 Numerical Example	28
	3.4 Conclusion	32
IV.	PERIODICALLY SUPPORTED INFINITE BEAM	
	4.1 Introduction	34
	4.2 Wave-Number Response Function of the Infinite Periodic Beam	35
	4.3 Numerical Example	45
	4.4 Conclusion	50
V.	MEMBRANE WITH RANDOM TENSION	
	5.1 Introduction	51

5.2 Wave-Number Response Function of Membrane 51

5.3 Numerical Example 65

5.4 Conclusion 71

VI. REYNOLDS STRESS ON A COMPLIANT SURFACE

6.1 Introduction 73

6.2 Theory 74

6.3 Periodically Supported Beam 88

6.4 Concluding Remarks 103

VII. GENERAL CONCLUSION 104

REFERENCES 106

I. INTRODUCTION

In recent years, there has been considerable interest in the response of panel systems to random pressure fields. An aircraft fuselage excited by boundary-layer turbulence or by the efflux of a jet engine is a good example. The objectives of such investigations [1-9] vary from minimizing structural fatigue damage to reducing noise radiation from the panel system to either outside or inside of the cabin. Recently, another important application has been suggested, namely, to design a panel system for the exterior of a vehicle such that the total skin-friction drag force over the vehicle is a minimum.

The typical panel system of an aircraft fuselage is a multi-span structure which is characterized by close clustering of natural frequencies in well-defined frequency bands. The usual normal mode formulation does not lead to practical results in this case, since it is almost impossible to calculate the normal modes of structures with a large number of spans due to close proximity of natural frequencies in each frequency band. However, if all the panels in a system are identically constructed, then the structural configuration is spatially periodic and the analysis can be greatly simplified. Two alternative methods are available to solve the response problem of such a spatially periodic structure: the transfer matrix technique [10-16] and the wave-propagation approach [17-21]. The computational simplicity of both methods is

achieved by utilizing the fact that the entire system is composed of identical subunits. Although these two methods are related [22], the transfer matrix technique is more suitable for analyzing a periodic structure with finite total length whereas the wave-propagation approach is more suitable for an infinite periodic structure.

In general, the spatial periodicity is no longer preserved when the excitation is included in the formulation, especially when the excitation is a random field. In principle, it is possible to express the total response under arbitrary excitation in terms of a fundamental solution which is the response due to one point-load on the structure. Mathematically, this fundamental solution is the Green's function and the total response can be represented as a convolution integral, but the actual calculation can become extremely tedious. One type of random excitation which does not destroy the spatial periodicity of the system is that which is convected as a frozen-pattern at a given velocity [14,19]. Known as Taylor's hypothesis, this is an assumption frequently made in the analysis of airplane response to atmospheric turbulence. Unfortunately, significant decays in the correlation of pressure field have been found in experimental measurements of boundary-layer turbulences [23-28]. Thus, calculations based on frozen-pattern models are just crude estimates as far as structural response to boundary-layer turbulence is concerned. Recently a scheme has been proposed [29-30] in which a decaying turbulence field is constructed

from frozen-pattern components, thus retaining the computational advantage of periodic structure models. This scheme (which we shall call the "turbulence decomposition scheme") will be used in this thesis and applications to structural response analyses will be discussed.

More specifically, the advantages of the turbulence decomposition scheme will be discussed in Chapter II by comparing to the conventional point-load analysis. In Chapter III the basic concepts of the turbulence decomposition scheme and its application to the structural response spectrum calculation will be developed using a simple model of an infinite unsupported beam exposed to a supersonic boundary-layer turbulence excitation. The effects of surrounding fluid will be taken into consideration. In Chapter IV the unsupported beam will be replaced by an infinite beam on evenly spaced supports which is a more realistic model of an actual aircraft panel system. The solutions will be compared with the experimental results. In Chapter V the case of a membrane with random structural properties will be considered and the effects on the spectral densities of the structural responses will be discussed. With potential applications to skin-friction drag reduction designs in mind, Chapter VI will be devoted to the analysis of the Reynolds stress in the boundary layer.

II. SPECTRAL ANALYSIS

2.1 Introduction

Measured cross-spectra of a turbulence field usually show some decay in the statistical correlation in addition to convection at a characteristic velocity [23-28]. Under such a random excitation the computation of structural response statistics becomes much more tedious than that which would be the case if the turbulence were convected without decay; i.e., convected as a frozen-pattern [14-19]. The conventional method of analysis is a point-load approach. As it will be shown in the next section, this method requires a numerical double integration to compute the cross-spectral density of the response of a one-dimensional structure. If the forcing field is a convected frozen-pattern field, then an alternative formulation will allow the cross-spectral density of the structural response to be computed without numerical integrations. However, because of the spatial decay in the measured turbulence spectra, the analysis for structural response based on the frozen-pattern assumption is just a crude estimate. The method to be discussed in this thesis retains the maximum computational benefits of the frozen-pattern analysis but at the same time the actually measured spectrum of turbulence field can be incorporated in the calculation. In this method a decaying turbulence will be treated as a superposition of frozen-pattern components so that the structural response can be superposed similarly. In the case of a one-dimensional

model, this method requires only a single integration instead of a double integration in the point-load analysis. The method will be called the "turbulence decomposition scheme" in the sequel.

To extend the turbulence decomposition scheme to a two-dimensional problem, the actual turbulence field is divided into strips which are running parallel to the x-axis, the direction of the mean flow. Each strip can then be decomposed into infinitely many frozen-pattern components as in the one-dimensional case. The total structural response is obtained by summing up the responses due to all the loading strips. In essense the point-load scheme is used in the across-flow direction whereas the frozen-pattern scheme is used in the along-flow direction.

In the following sections the one-dimensional case will be discussed first and then the two-dimensional structure. Furthermore, a general treatment of random structural properties will be included in the formulation of the two-dimensional problem.

2.2 The Statistical Properties of the Excitation

Measured frequency cross-spectra for pressure variations in a turbulent boundary layer with respect to a fixed frame of reference have the general form of

$$\bar{\Phi}_p(\xi,\eta,\omega) = \bar{\Phi}_p(0,0,\omega)\psi_1(\xi)\psi_2(\eta)\exp(-i\omega\xi/U_c) \qquad (2.1)$$

where U_c is a characteristic velocity, and ψ_1 and ψ_2 are non-negative definite even functions of ξ and η, respectively. These two functions have an absolute maximum equal to one at the origin and they approach to zero at large absolute values of the argument. The general form, Eq. (2.1), is sometimes attributed to Corcos [23]. A number of researchers have reported curve-fitted results for $\bar{\Phi}_p(0,0,\omega)$, $\psi_1(\xi)$ and $\psi_2(\eta)$. For representative works we cite the papers by Bull [24], Willmarth and Wooldridge [25], and Maestrello, et al [26-28]. Implicit in Eq. (2.1) is that a real turbulence is not a frozen one. We note that the above pressure spectrum reduces to that of a plane wave field if $\psi_2(\eta) = 1$, and it would correspond to a frozen-pattern turbulence if $\psi_1(\xi) = 1$.

For additional physical insight and later use in sample calculations, two measured spectra are given below:

For a subsonic boundary layer [26,27]:

$$\bar{\Phi}_p(0,0,\omega) = \frac{1}{2}\frac{\delta^*}{U_\infty}\sum_{n=1}^{3} A_n\, e^{-\frac{\delta^*}{U_\infty}K_n|\omega|} \tag{2.2}$$

$$\psi_1(\xi) = \exp\left(-\frac{|\xi|}{U_c\theta}\right) \tag{2.3}$$

$$\psi_2(\eta) = \exp\left(-\frac{|\eta|}{\alpha\delta^*}\right) \tag{2.4}$$

$A_1 = 0.240$ $\qquad$ $K_1 = 0.470$

$A_2 = 1.08$ $\qquad$ $K_2 = 3.0$

$A_3 = 1.80$ $\qquad$ $K_3 = 14.0$

$\alpha = 2$

$$\theta = -\ (1.24 \times 10^{-3})\ (U_\infty/a_1) + 1.15 \times 10^{-3} \text{ sec}$$

$$U_c = 0.8\ U_\infty$$

where U_∞ is the free-stream velocity, a_1 denotes the speed of sound in the field, δ^* represents the boundary-layer displacement thickness, and θ is the average eddy lifetime.

For a supersonic boundary layer [28]:

$$\bar{\Phi}_p(0,0,\omega) = \frac{1}{2}\frac{\delta}{U_\infty}\sum_{n=1}^{4} A_n\, e^{-\frac{\delta}{U_\infty}K_n|\omega|} \tag{2.5}$$

$$\psi_1(\xi) = \exp\left(-\frac{|\xi|}{\alpha_1\delta}\right) \tag{2.6}$$

$$\psi_2(\eta) = \exp\left(-\frac{|\eta|}{\alpha_2\delta}\right) \tag{2.7}$$

$A_1 = 4.4 \times 10^{-2}$ $\qquad$ $K_1 = 5.78 \times 10^{-2}$

$A_2 = 7.5 \times 10^{-2}$ $\qquad$ $K_2 = 2.43 \times 10^{-1}$

$A_3 = -9.3 \times 10^{-2}$ $\qquad$ $K_3 = 1.12$

$A_4 = -2.5 \times 10^{-2}$ $\qquad$ $K_4 = 11.57$

$\alpha_1 = 3$ $\qquad$ $\alpha_2 = 0.26$

$U_c = 0.75\ U_\infty$

Where δ is the boundary-layer thickness which is defined as the distance from the boundary at which the average value of the turbulence velocity reaches $0.99\ U_\infty$.

2.3 Point-Load Analysis

Consider a unit concentrated load at $x = \xi$ on a one-dimensional structure where x is measured along the structure, parallel to the flow direction. We obtain a frequency response function $\tilde{H}(x,\xi,\omega)$ by solving the equation

$$\mathcal{L}\{\tilde{H}(x,\xi,\omega)\, e^{i\omega t}\} = \delta(x-\xi)\, e^{i\omega t} \tag{2.8}$$

where $\mathcal{L}\{\ \}$ represents a linear differential operator in x and t, and $\delta(\ )$ is a Dirac delta function. Then, the cross-spectral density of the structural response $\Phi_w(x_1,x_2,\omega)$ is calculated from

$$\Phi_w(x_1,x_2,\omega) = \int_0^{\ell}\int_0^{\ell} \tilde{H}(x_1,\xi_1,\omega)\, \tilde{H}^*(x_2,\xi_2,\omega)\, \Phi_p(\xi_1-\xi_2,\omega)\, d\xi_1 d\xi_2 \tag{2.9}$$

where $\Phi_p(\xi_1-\xi_2,\omega)$ is the cross-spectrum of the pressure field, ℓ is the length of the structure under consideration, and an asterisk denotes the complex conjugate. It is assumed that the loading is a spatially homogeneous random process; therefore, the cross-spectrum Φ_p depends on $\xi_1-\xi_2$. Although this method is quite straightforward, long computer time is required to carry out the double integration in Eq. (2.9).

2.4 Frozen-Pattern Analysis

If the pressure is truly of a frozen type and is convected at a constant velocity U_c in the positive x-direc-

tion, then it is a random function of $x - U_c t$. Such a random function can be expressed as a Fourier-Stieltjes integral as follows:

$$p(x - U_c t) = \int_{-\infty}^{\infty} e^{i(\omega t - kx)} \, dF(k) \tag{2.10}$$

where the frequency ω and the wave-number k are related to the convection speed U_c as $\omega/k = U_c$. It is known from the random process theory that

$$E\{dF(k_1) \, dF^*(k_2)\} = S_p(k_1) \, \delta(k_1 - k_2) \, dk_1 dk_2 \tag{2.11}$$

where $E\{\ \}$ represents the ensemble average, and $S_p(k)$ is the wave-number spectrum in a coordinate frame moving at the velocity U_c (referred to as the moving frame in the sequel).

The cross-correlation function $E\{p(x_1 - U_c t_1) \, p(x_2 - U_c t_2)\}$ of the pressure, referred to the fixed frame, can be calculated simply by use of Eqs. (2.10) and (2.11). This function, denoted by R_p, depends only on $\xi - U_c \tau$ where $\xi = x_1 - x_2$ and $\tau = t_1 - t_2$, and it is related to the moving-frame wave-number spectrum $S_p(k)$ as follows:

$$R_p(\xi - U_c \tau) = \int_{-\infty}^{\infty} e^{ik(U_c \tau - \xi)} \, S_p(k) \, dk \tag{2.12}$$

If a Riemann-Fourier transform is taken of Eq. (2.12) we obtain the fixed-frame frequency cross-spectrum of p:

$$\Phi_p(\xi,\omega) = \frac{1}{2\pi}\int_{-\infty}^{\infty} R_p(\xi - U_c\tau)\, e^{-i\omega\tau}\, d\tau$$

$$= \frac{1}{|U_c|} S_p\left(\frac{\omega}{U_c}\right) e^{-i(\omega/U_c)\xi} \qquad (2.13)$$

Equation (2.13) shows that the fixed-frame frequency cross-spectrum of a frozen-pattern turbulence has a special form where ξ appears only in the imaginary exponent. This equation also provides a simple formula to convert from $S_p(k)$ to $\Phi_p(\xi,\omega)$. Conversely, to convert from $\Phi_p(\xi,\omega)$ to $S_p(k)$:

$$S_p(k) = |U_c|\, \Phi_p(0,kU_c) \qquad (2.14)$$

Evaluated at $\xi = 0$ the cross-spectrum $\Phi_p(\xi,\omega)$ reduces, of course, to the usual spectrum. We emphasize that Eqs. (2.13) and (2.14) are valid only if the turbulence is strictly of a frozen-pattern, and is convected at speed U_c.

Equation (2.10) suggests that the structural response to a frozen-pattern turbulence can be constructed from a fundamental solution where the excitation is just a convected sinusoidal pattern of unit amplitude. Thus, let $H(x,k)\exp(i\omega t)$ be the steady-state solution for

$$\mathcal{L}\{H(x,k)\exp(i\omega t)\} = \exp[i(\omega t - kx)] \qquad (2.15)$$

Of course, this solution must satisfy all the necessary boundary conditions. Then the solution to

$$\mathcal{L}\{w(x,t)\} = p(x - U_c t) \qquad (2.16)$$

after reaching stochastic stationality, may be expressed as

$$w(x,t) = \int_{-\infty}^{\infty} H(x,k)\, \exp(i\omega t)\, dF(k)$$

$$= \int_{-\infty}^{\infty} H(x,k)\, \exp(iU_c kt)\, dF(k) \qquad (2.17)$$

It follows that the cross-correlation function of the structural response is

$$E\{w(x_1,t_1)\, w(x_2,t_2)\}$$

$$= \iint_{-\infty}^{\infty} H(x_1,k_1)\, H^*(x_2,k_2)\, e^{iU_c(k_1 t_1 - k_2 t_2)}$$

$$S_p(k_1)\, \delta(k_1 - k_2)\, dk_1 dk_2$$

$$= \int_{-\infty}^{\infty} H(x_1,k)\, H^*(x_2,k)\, e^{iU_c k(t_1 - t_2)} S_p(k)\, dk \qquad (2.18)$$

As expected, this correlation function is dependent only on $t_1 - t_2$. If it is desired to calculate this correlation function in the frequency domain, we may substitute Eq. (2.14) into Eq. (2.18) and change $U_c k$ to ω:

$$E\{w(x_1,t_1)\, w(x_2,t_2)\}$$

$$= \int_{-\infty}^{\infty} H(x_1,\omega/U_c)\, H^*(x_2,\omega/U_c)\, e^{i\omega(t_1 - t_2)} \Phi_p(0,\omega) d\omega \qquad (2.19)$$

In terms of the input and output spectra the relations are extremely simple and illuminative; they are:

in the wave-number domain:

$$S_w(x_1,x_2;k) = H(x_1,k)\, H^*(x_2,k)\, S_p(k) \qquad (2.20)$$

in the frequency domain:

$$\Phi_w(x_1,x_2;\omega) = H(x_1,\omega/U_c)\, H^*(x_2,\omega/U_c)\, \Phi_p(o,\omega) \qquad (2.21)$$

When $x_1 = x_2$ these formulas reduce to those for the usual spectra, and they have the same form as the well-known result for a single degree of freedom system in the random vibration theory.

It is appropriate to call the H function in Eqs. (2.20) and (2.21) the wave-number response function for convected frozen load to distinguish it from the $\tilde{H}$ function in Eq. (2.9) which is the frequency response function for point load.

The advantage of the frozen-pattern assumption is clear. To obtain the cross-spectrum of the response, no integration is required under this assumption while a double integration is needed in the point-load analysis, Eq. (2.9). Unfortunately, significant decays in the correlation have been found in experimental measurements of boundary-layer turbulences. Thus, correlations based on frozen-pattern models are just crude estimates, at least for the calculation of structural responses to the boundary-layer turbulence.

2.5 Turbulence Decomposition Scheme - One-Dimensional Case

In the one-dimensional case measured frequency cross-spectra have the general form of

$$\bar{\Phi}_p(\xi,\omega) = \bar{\Phi}_p(0,\omega)\ \psi(\xi)\ \exp(-i\omega\xi/U_c) \tag{2.22}$$

which is reduced from Eq. (2.1). Implicit in Eq. (2.22) is that a real turbulence is not a frozen-pattern one.

To obtain a theoretical spectrum consistent with Eq. (2.22) the following representation of a general turbulence pressure is proposed:

$$p(x,t) = \int_{-\infty}^{\infty} \hat{p}(x - ut)\ dG(u) \tag{2.23}$$

Eq. (2.23) implies that $p(x,t)$ is a superposition of infinitely many frozen-pattern components, each having a real random amplitude $dG(u)$ and a convection velocity u. Such velocities can assume either positive or negative values. Of course, each frozen-pattern component can, again, be decomposed into sinusoids. Thus

$$p(x,t) = \iint_{-\infty}^{\infty} e^{i(ukt - kx)}\ dF(k,u)\ dG(u) \tag{2.24}$$

and its fixed-frame correlation is

$$E\{p(x_1,t_1)\ p(x_2,t_2)\}$$

$$= \iiiint_{-\infty}^{\infty} \exp[i(u_1 k_1 t_1 - u_2 k_2 t_2) - i(k_1 x_1 - k_2 x_2)]$$

$$E\{dF(k_1,u_1)\ dF^*(k_2,u_2)\ dG(u_1)\ dG(u_2)\} \qquad (2.25)$$

In order that this correlation function may depend only on $\xi = x_1 - x_2$ and $\tau = t_1 - t_2$, which we shall assume to be true, the ensemble average under the integral sign in Eq. (2.25) must have the form

$$E\{dF(k_1,u_1)\ dF^*(k_2,u_2)\ dG(u_1)\ dG(u_2)\}$$

$$= S_p(k_1,u_1)\ \delta(k_1 - k_2)\ \delta(u_1 - u_2)\ dk_1 dk_2 du_1 du_2 \qquad (2.26)$$

Substitution of Eq. (2.26) into Eq. (2.25) results in

$$R_p(\xi,\tau) = \iint_{-\infty}^{\infty} e^{i(ku\tau - k\xi)}\ S_p(k,u)\ dk\ du \qquad (2.27)$$

We now apply a Fourier transformation to obtain the fixed-frame frequency spectrum

$$\Phi_p(\xi,\omega) = \frac{1}{2\pi}\int_{-\infty}^{\infty} R_p(\xi,\tau)\ e^{-i\omega\tau}\ d\tau$$

$$= \int_{-\infty}^{\infty} \frac{1}{|u|}\, e^{-i\omega\xi/u}\ S_p\left(\frac{\omega}{u},u\right)\ du \qquad (2.28)$$

Clearly Eq. (2.28) is a generalization of Eq. (2.13).

To compare Eqs. (2.28) and (2.22), the latter is Fourier-transformed to yield

$$\frac{1}{2\pi}\int_{-\infty}^{\infty}\bar{\Phi}_p(\xi,\omega)\ e^{i\xi\alpha}\ d\xi = \bar{\Phi}_p(0,\omega)\ \Psi(\alpha - \frac{\omega}{U_c}) \tag{2.29}$$

where

$$\Psi(v) = \frac{1}{2\pi}\int_{-\infty}^{\infty}\psi(\xi)\ e^{i\xi v}\ d\xi \tag{2.30}$$

Therefore,

$$\bar{\Phi}_p(\xi,\omega) = \bar{\Phi}_p(0,\omega)\int_{-\infty}^{\infty}\Psi(\alpha - \frac{\omega}{U_c})\ e^{-i\alpha\xi}\ d\alpha \tag{2.31}$$

Letting $\alpha = \omega/u$, we obtain

$$\bar{\Phi}_p(\xi,\omega) = \bar{\Phi}_p(0,\omega)\int_{-\infty}^{\infty}\left|\frac{\omega}{u^2}\right|\ \Psi(\frac{\omega}{u} - \frac{\omega}{U_c})\ e^{-i\omega\xi/u}\ du \tag{2.32}$$

Then equating Φ_p and $\bar{\Phi}_p$ we find a formula to compute $S_p(\omega/u,u)$ as follows:

$$S_p(\frac{\omega}{u},u) = \left|\frac{\omega}{u}\right|\ \Psi(\frac{\omega}{u} - \frac{\omega}{U_c})\ \bar{\Phi}_p(0,\omega)$$

$$= \left|\frac{\omega}{2\pi u}\right|\ \bar{\Phi}_p(0,\omega)\int_{-\infty}^{\infty}\psi(\xi)\ \exp[i\xi(\frac{\omega}{u} - \frac{\omega}{U_c})]\ d\xi \tag{2.33}$$

The frequency cross-spectrum for the structural response can be obtained by a similar superposition. Thus by a generalization of Eq. (2.21),

$$\Phi_w(x_1,x_2,\omega) = \int_{-\infty}^{\infty}\frac{1}{|u|}H(x_1,\frac{\omega}{u})\ H^*(x_2,\frac{\omega}{u})\ S_p(\frac{\omega}{u},u)\ du \tag{2.34}$$

Or, letting $k = \omega/u$,

$$\Phi_w(x_1,x_2;\omega) = \int_{-\infty}^{\infty} \frac{1}{|k|} H(x_1,k)\ H^*(x_2,k)\ S_p(k,\frac{\omega}{k})\ dk \quad (2.35)$$

Now, since

$$S_p(k,\frac{\omega}{k}) = |k|\ \bar{\Phi}_p(0,\omega)\ \Psi(k - \frac{\omega}{U_c})$$

we obtain a very simple result

$$\Phi_w(x_1,x_2;\omega) = \bar{\Phi}_p(0,\omega) \int_{-\infty}^{\infty} H(x_1,k)$$

$$H^*(x_2,k)\ \Psi(k - \frac{\omega}{U_c})\ dk \quad (2.36)$$

As a check we note that when the turbulence is frozen-pattern, $\psi(\xi) = 1$ and

$$\Psi(v) = \delta(v) \quad (2.37)$$

then Eq. (2.36) reduces to the same form as Eq.(2.21).
In the case when the structural acceleration response is the main concern of the problem, Eq. (2.36) is changed to

$$\Phi_{\ddot{w}}(x_1,x_2;\omega) = \omega^4\ \bar{\Phi}_p(0,\omega) \int_{-\infty}^{\infty} H(x_1,k)$$

$$H^*(x_2,k)\ \Psi(k - \frac{\omega}{U_c})\ dk \quad (2.38)$$

2.6 Turbulence Decomposition Scheme - Two-Dimensional Case

Generalization of the results obtained in the last section to a two-dimensional pressure field is straightforward.

Assuming that such a pressure field can be decomposed into frozen-pattern components, we have

$$p(x,y,t) = \int_{-\infty}^{\infty} \hat{p}(x - ut,y)\, dG(u) \tag{2.39}$$

where both $\hat{p}$ and G are random functions and $\hat{p}$ is a frozen-pattern component of p. Each component pressure $\hat{p}$ can again be constructed from frozen-pattern sinusoids. Thus

$$p(x,y,t) = \iint_{-\infty}^{\infty} e^{i(ukt - kx)}\, dF(k,u,y)\, dG(u) \tag{2.40}$$

In order that the cross-correlation of the random pressure $E\{p(x_1,y_1,t_1)\ p(x_2,y_2,t_2)\}$ is dependent only on $\xi = x_1 - x_2$, $\eta = y_1 - y_2$, and $\tau = t_1 - t_2$, the cross-correlation of dFdG must have the form

$$\begin{aligned} &E\{dF(k_1,u_1,y_1)\ dF^*(k_2,u_2,y_2)\ dG(u_1)\ dG(u_2)\} \\ &= S_p(k_1,u_1,\eta)\ \delta(k_1 - k_2)\ \delta(u_1 - u_2) \\ &\quad dk_1\ dk_2\ du_1\ du_2 \end{aligned} \tag{2.41}$$

Then, it can be shown that the cross-spectrum of p has the form

$$\Phi_p(\xi,\eta,\omega) = \int_{-\infty}^{\infty} \frac{1}{|u|} S_p\left(\frac{\omega}{u},u,\eta\right) e^{-i\omega\xi/u}\, du \tag{2.42}$$

Equating Eq. (2.42) with the general form of the measured turbulent pressure spectra, Eq. (2.1), results in

$$S_p(\frac{\omega}{u},u,\eta) = |\frac{\omega}{u}|\Psi_1(\frac{\omega}{u} - \frac{\omega}{U_c})\ \bar{\Phi}_p(0,0,\omega)\ \psi_2(\eta) \qquad (2.43)$$

where Ψ_1 is the Fourier transform of ψ_1; i.e.,

$$\Psi_1(v) = \frac{1}{2\pi}\int_{-\infty}^{\infty} \psi_1(\xi)\ e^{i\xi v}\ d\xi \qquad (2.44)$$

It is clear from Eq. (2.40) that, in this case, the structural response can also be constructed from a fundamental solution which is obtained by letting the excitation be some suitable frozen-pattern sinusoid. Denote this fundamental solution by $H(x,k,y,y',\omega)$ and let $H \exp(i\omega t)$ be the steady-state solution for

$$\mathcal{L}\{H(x,k,y,y',\omega)\ e^{i\omega t}\} = e^{i(\omega t - kx)}\delta(y - y') \qquad (2.45)$$

where $\mathcal{L}$ represents a linear operator in x, y and t. The physical meaning of H is self-explanatory; it is the complex amplitude of the steady-state structural response at (x,y) due to a strip of excitation along $y = y'$ which is convecting in the x-direction. Then, the solution to

$$\mathcal{L}\{w(x,y,t)\} = p(x,y,t) \qquad (2.46)$$

after reaching the stochastic stationality, may be expressed as

$$w(x,y,t) = \int_0^b dy' \iint_{-\infty}^{\infty} H(x,k,y,y',\omega)\ e^{i\omega t}$$

$$dF(k,\frac{\omega}{k},y')\ dG(\frac{\omega}{k})$$

$$= \int_0^b dy' \iint_{-\infty}^{\infty} H(x,k,y,y',ku)\, e^{ikut}\, dF(k,u,y')\, dG(u) \quad (2.47)$$

where b is the width of the structure in the y-direction. The cross-correlation of the response is, therefore, obtained as follows:

$$E[w(x_1,y_1,t_1)\, w(x_2,y_2,t_2)]$$

$$= \int_0^b\int dy_1'dy_2' \iiiiint_{-\infty}^{\infty} H(x_1,k_1,y_1,y_1',k_1u_1)$$

$$H^*(x_2,k_2,y_2,y_2',k_2u_2)\, e^{i(k_1u_1t_1 - k_2u_2t_2)}$$

$$S_p(k_1,u_1,y_1' - y_2')\, \delta(k_1 - k_2)\, \delta(u_1 - u_2)$$

$$dk_1\, dk_2\, du_1\, du_2$$

$$= \int_0^b\int dy_1'dy_2' \iint_{-\infty}^{\infty} H(x_1,k,y_1,y_1',ku)\, H^*(x_2,k,y_2,y_2',ku)$$

$$e^{ik u\tau}\, S_p(k,u,y_1' - y_2')\, dk\, du \quad (2.48)$$

Substituting Eq. (2.43) into Eq. (2.48) and applying a Fourier transformation, we obtain the cross-spectrum of the structural response

$$\Phi_w(x_1,x_2,y_1,y_2,\omega)$$

$$= \overline{\Phi}_p(0,0,\omega) \int_0^b\int dy_1'dy_2' \int_{-\infty}^{\infty} H(x_1,k,y_1,y_1',\omega)$$

$$H^*(x_2,k,y_2,y_2',\omega)\ \Psi_1(k - \frac{\omega}{U_c})\ \psi_2(y_1' - y_2')\ dk \qquad (2.49)$$

The reason for not using the same decomposition scheme in the y-direction as that for the x-direction is the absence of true trend of convection which can be seen in Eq. (2.1). Therefore, the correlation length of the random forcing field in the y-direction seldom extends beyond one panel and the structural response can be computed quite accurately using a structural model consisting of just one row of panels running in the x-direction. For such a model the usual Levy series representation of the y-direction response is adequate and the double integration on y_1' and y_2' in Eq. (2.49) can be carried out without difficulty.

Thus far, the structural properties are assumed to be deterministic; therefore, the frequency response function H is a deterministic function. Sometimes it may be of interest to include the effects of random variability of the structural properties in the calculation, then H becomes a random process. In this case the cross-correlation of the structural response becomes

$$E\{w(x_1,y_1,t_1)\ w(x_2,y_2,t_2)\}$$

$$= \int_0^b\int dy_1'dy_2' \int_{-\infty}^{\infty}\int\int\int E\{H(x_1,k_1,y_1,y_1',k_1u_1)$$

$$H^*(x_2,k_2,y_2,y_2',k_2u_2)\ dF(k_1,u_1,y_1')\ dF^*(k_2,u_2,y_2')$$

$$dG(u_1)\ dG(u_2)\}\ e^{i(k_1u_1t_1 - k_2u_2t_2)} \qquad (2.50)$$

If the structural properties and the turbulence properties are independent of each other, which is a reasonable assumption, the ensemble average inside the integral of Eq. (2.50) is separable. Again, using Eq. (2.41) we have

$$E\{w(x_1,y_1,t_1)\ w(x_2,y_2,t_2)\}$$

$$= \int_0^b\int_0^b dy_1' dy_2' \int_{-\infty}^{\infty} E\{H(x_1,k,y_1,y_1',ku)\ H^*(x_2,k,y_2,y_2',ku)\}$$

$$S_p(k,u,y_1' - y_2')\ e^{iku\tau}\ dk\ du \qquad (2.51)$$

The cross-spectrum of the structural response is obtained by a Fourier transformation of Eq. (2.51), resulting in

$$\Phi_w(x_1,x_2,y_1,y_2,\omega)$$

$$= \bar{\Phi}_p(0,0,\omega) \int_0^b\int_0^b dy_1' dy_2' \int_{-\infty}^{\infty} E\{H(x_1,k,y_1,y_1',\omega)$$

$$H^*(x_2,k,y_2,y_2',\omega)\}\ \Psi_1(k - \frac{\omega}{U_c})\ \psi_2(y_1' - y_2')\ dk \qquad (2.52)$$

2.7 Conclusion

The turbulence decomposition scheme has been discussed and compared with the conventional point-load approach. It has been shown that a decaying and convecting turbulence pressure field can be constructed from frozen-pattern components, each having a different convection velocity, and that this new scheme simplifies greatly the analyses of random properties of structural responses under the excitation of boundary-layer turbulence pressure. In paticular, only a single integration

is required to compute the cross-spectrum of the structural response instead of a double integration in the point-load approach. The integration involves a wave-number response function which is the response of the structure to a unit convected sinusoid. In the following chapters applications of this scheme will be discussed for some structural configurations and flow field problems.

III. UNSUPPORTED INFINITE BEAM

3.1 Introduction

A simple model which, nevertheless, retains most important features of aircraft panels in a boundary-layer environment is the infinite beam shown in Fig.3.1. The beam is backed on the lower side by a space of depth d which is filled with an initially quiescent fluid of density ρ_2 and sound speed a_2. On the upper side the beam is exposed to the excitation of a supersonic boundary-layer turbulent pressure p. The fluid on the upper side of the beam which carries the turbulence has a free-stream velocity U_∞, density ρ_1, and sound speed a_1. An actual panel system of an aircraft is reinforced by stringers and frames so that this unsupported beam is not a good representation at low frequency range. However, at high frequencies, the turbulence eddy size is much smaller than individual panels. Then the effect of the constraints at the stringers and frames becomes negligible. In any case the infinite beam model is an ideal one which can be used to show the utility of the turbulence decomposition method as well as the structure-fluid interaction without the burden of mathematical complexities.

3.2 Wave-Number Response Function of the Infinite Unsupported Beam

As the beam responds to the excitation pressure p(x,t)

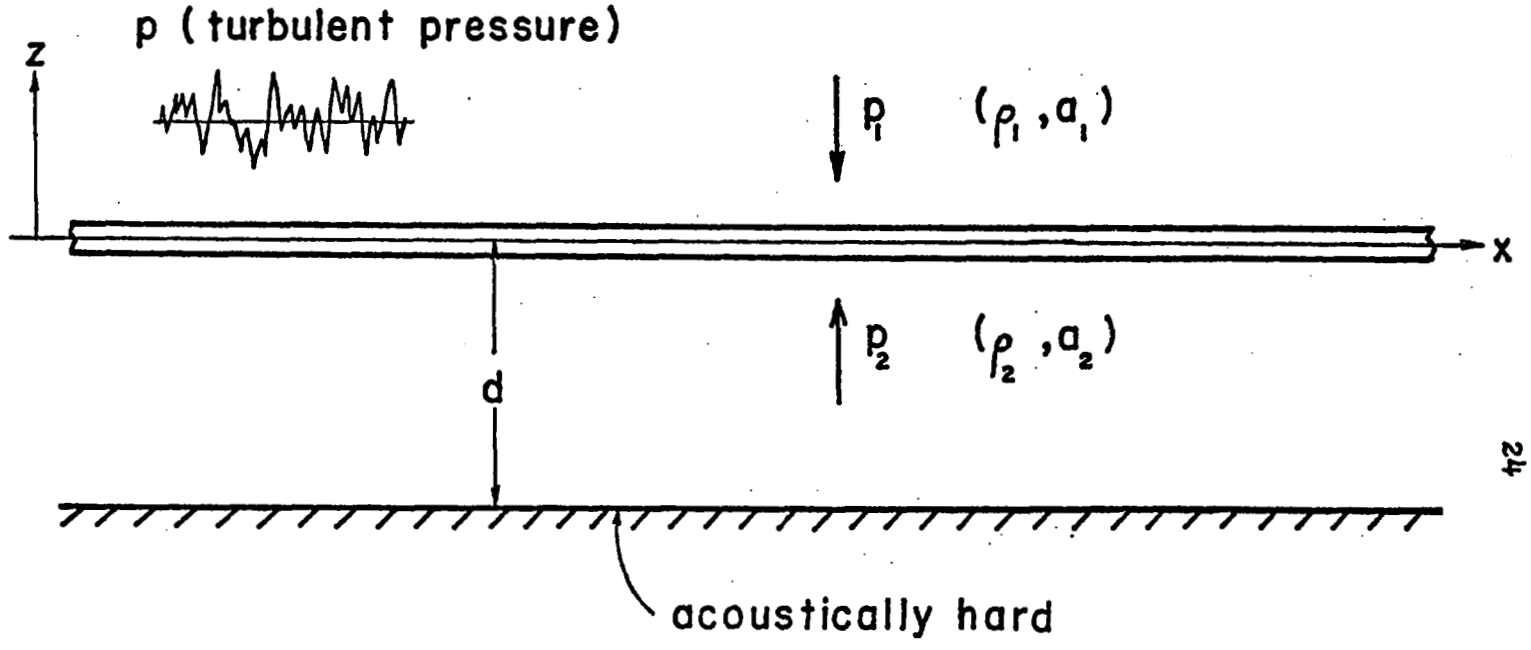

Fig. 3.1 An unsupported infinite beam under the excitation of boundary-layer turbulence

its motion will generate additional pressures in the fluid media on the upper and lower sides. Denoting these generated pressures by p_1 and p_2, respectively, the governing equation of the beam motion is given by

$$EI \frac{\partial^4 w}{\partial x^4} + m \frac{\partial^2 w}{\partial t^2} = p + (p_1 - p_2)_{z=0} \tag{3.1}$$

where E denotes the Young's modulus, I is the moment of inertia, m is the mass per unit length of the beam.

For the purpose of determining the wave-number response function, H(x,k), the turbulent pressure p should be replaced by $\exp[i(\omega t - kx)]$ and the structural response w equated with $H(x,k) \exp(i\omega t) = A(k) \exp(-ikx) \exp(i\omega t)$. Furthermore, we shall make the usual approximation that p_1 can be calculated without regard to the presence of the turbulence. Then p_1 is governed by the equation

$$\left(\frac{\partial}{\partial t} + U_\infty \frac{\partial}{\partial x}\right)^2 p_1 - a_1^2 \left(\frac{\partial^2}{\partial x^2} + \frac{\partial^2}{\partial z^2}\right) p_1 = 0 \tag{3.2}$$

and subject to the conditions that p_1 can propagate only in the positive z-domain, and that

$$\left(\frac{\partial p_1}{\partial z}\right)_{z=0} = \rho_1 \left(\frac{\partial}{\partial t} + U_\infty \frac{\partial}{\partial x}\right)^2 A(k)\, e^{i(\omega t - kx)} \tag{3.3}$$

The solution for p_1, when evaluated at z = 0, is known to be [31]

$$(p_1)_{z=0} = -i\rho_1 a_1 \frac{k(\omega/k - U_\infty)^2}{[(\omega/k - U_\infty)^2 - a_1^2]^{\frac{1}{2}}} A(k)\, e^{i(\omega t - kx)} \tag{3.4}$$

Some comments about Eq. (3.4) are in order: (1) ω/k is the speed at which the structural motion $A(k)\exp[i(\omega t - kx)]$ is propagated along the beam. (2) A structural motion generates no pressure in the adjacent fluid medium if it is propagated at the same velocity as that of the fluid medium (the case of $\omega/k = U_\infty$). (3) Theoretically, the generated pressure attains an infinite amplitude when the propagation velocity of the structural motion relative to the medium is equal to the speed of sound (the case of $|\omega/k - U_\infty| = a_1$, the shock-wave effect). (4) When this relative velocity is less than the speed of sound; i.e., $|\omega/k - U_\infty| < a_1$, the generated pressure should provide additional inertia for the structural motion (the apparent mass effect); therefore, a negative imaginary value should be given to the square-root $[(\omega/k - U_\infty)^2 - a_1^2]^{\frac{1}{2}}$ in the calculation.

The pressure generated on the lower side of the beam is governed by the equation

$$\frac{\partial^2 p_2}{\partial t^2} - a_2^2\left(\frac{\partial^2}{\partial x^2} + \frac{\partial^2}{\partial z^2}\right) p_2 = 0 \qquad (3.5)$$

and subject to the conditions

$$\frac{\partial p_2}{\partial z} = 0 \qquad \text{at } z = -d \qquad (3.6)$$

and

$$\frac{\partial p_2}{\partial z} = -\rho_2\omega^2 A(k)\, e^{i(\omega t - kx)} \qquad \text{at } z = 0 \qquad (3.7)$$

The solution for p_2, when evaluated at $z = 0$, is given by

$$(p_2)_{z=0} = \rho_2\omega^2 \frac{\cot(\gamma d)}{\gamma} A(k)\, e^{i(\omega t - kx)} \tag{3.8}$$

where

$$\gamma^2 = \left(\frac{\omega}{a_2}\right)^2 - k^2 \tag{3.9}$$

For small d (shallow cavity) and $\gamma^2 > 0$, this pressure provides additional stiffness on the structural motion but for certain ranges of d value it can change to an added mass. When $\gamma^2 < 0$, γ becomes imaginary in which case

$$\frac{\cot(\gamma d)}{\gamma} = -\frac{\coth|\gamma d|}{|\gamma|} \tag{3.10}$$

Again, the p_2 term has the effect of an added mass on the structural response.

Eqs. (3.4) and (3.8) can now be substituted into Eq. (3.1) to find A(k) and, therefore, H(x,k), recalling that p must be replaced by $\exp[i(\omega t - kx)]$ and w by $A(k)\exp[i(\omega t-kx)]$. The result may be expressed as

$$\begin{aligned} H(x,k) &= A(k)\, e^{-ikx} \\ &= \left\{EIk^4 - m\omega^2 + i\rho_1 a_1 \frac{k(\omega/k - U_\infty)^2}{[(\omega/k - U_\infty)^2 - a_1^2]^{\frac{1}{2}}}\right. \\ &\quad \left. + \rho_2\omega^2 \frac{\cot(\gamma d)}{\gamma}\right\}^{-1} e^{-ikx} \end{aligned} \tag{3.11}$$

This wave-number response function H can now be substituted into Eq. (2.36) to obtain the cross-spectral density of the structural displacement response.

3.3 Numerical Example

Numerical computations have been carried out for the frequency spectrum (i.e., when $x_1 = x_2$ in Eq. (2.36)) of the structural response using the following physical data:

properties of the beam:

EI (bending rigidity) = 3.935×10^4 N-m^2

m (mass per unit length) = 9.746 Kg/m

properties of the surrounding fluid media:

$\rho_1 = \rho_2 = \rho$ (air density) = 0.11015 Kg/m^3

$a_1 = a_2 = a$ (speed of sound) = 261.6 m/sec

U_∞ (free-stream velocity on upper side of beam) = 575.6 m/sec

d (cavity depth) = 0.1178 m

properties of the supersonic boundary-layer turbulence pressure [28]:

$$\bar{\Phi}_p(0,\omega) = \text{spectral density} = \frac{1}{2}\frac{\delta}{U_\infty}\sum_{n=1}^{4} A_n\, e^{-K_n(|\omega|\delta/U_\infty)}$$

$$\psi(\xi) = \text{decay factor} = \exp\left(-\frac{|\xi|}{\alpha\delta}\right)$$

U_c (characteristic convection velocity of the turbulence) = $0.75\, U_\infty$

$$\Psi\left(k - \frac{\omega}{U_c}\right) = \frac{1}{\pi\alpha\delta\left[(\alpha\delta)^{-2} + (k - \omega/U_c)^2\right]}$$

δ (boundary-layer thickness) = 0.279 m

experimentally determined constants

$\alpha = 3$

$A_1 = 4.4 \times 10^{-2}$ $\quad K_1 = 5.78 \times 10^{-2}$

$A_2 = 7.5 \times 10^{-2}$ $\quad K_2 = 2.43 \times 10^{-1}$

$A_3 = -9.3 \times 10^{-2}$ $\quad K_3 = 1.12$

$A_4 = -2.5 \times 10^{-2}$ $\quad K_4 = 11.57$

Fig.3.2 shows the computed displacement frequency spectrum of the structural response under the assumption of a truly frozen-pattern turbulence ($\psi(\xi) = 1$). There appears only one peak around 475 Hz and the value of spectrum decreases rapidly as the frequency increases. The existence of the peak can be explained as follows: In the absence of surrounding fluids, the wave number of the free structural motion would be $(m\omega^2/EI)^{\frac{1}{4}}$. The wave number of the frozen-pattern turbulence, k, is related to the circular frequency ω by $k = \omega/U_c$. A resonance (called coincidence) occurs when these two wave numbers are equal [32]. In the present case this coincidence frequency is found at 466 Hz. Therefore, the peak in Fig. 3.2 results from the coincidence of the wave numbers of the frozen-pattern turbulence and the free structural motion. The small difference between the peak frequency in Fig. 3.2 and the estimated value above comes from the effect of the surrounding fluids on the structural response.

Fig. 3.3 shows the spectrum of the structural displacement response when the measured spectrum of the turbulence pressure field is used in the computation. This spectral density has many peaks in contrast with only one peak in the

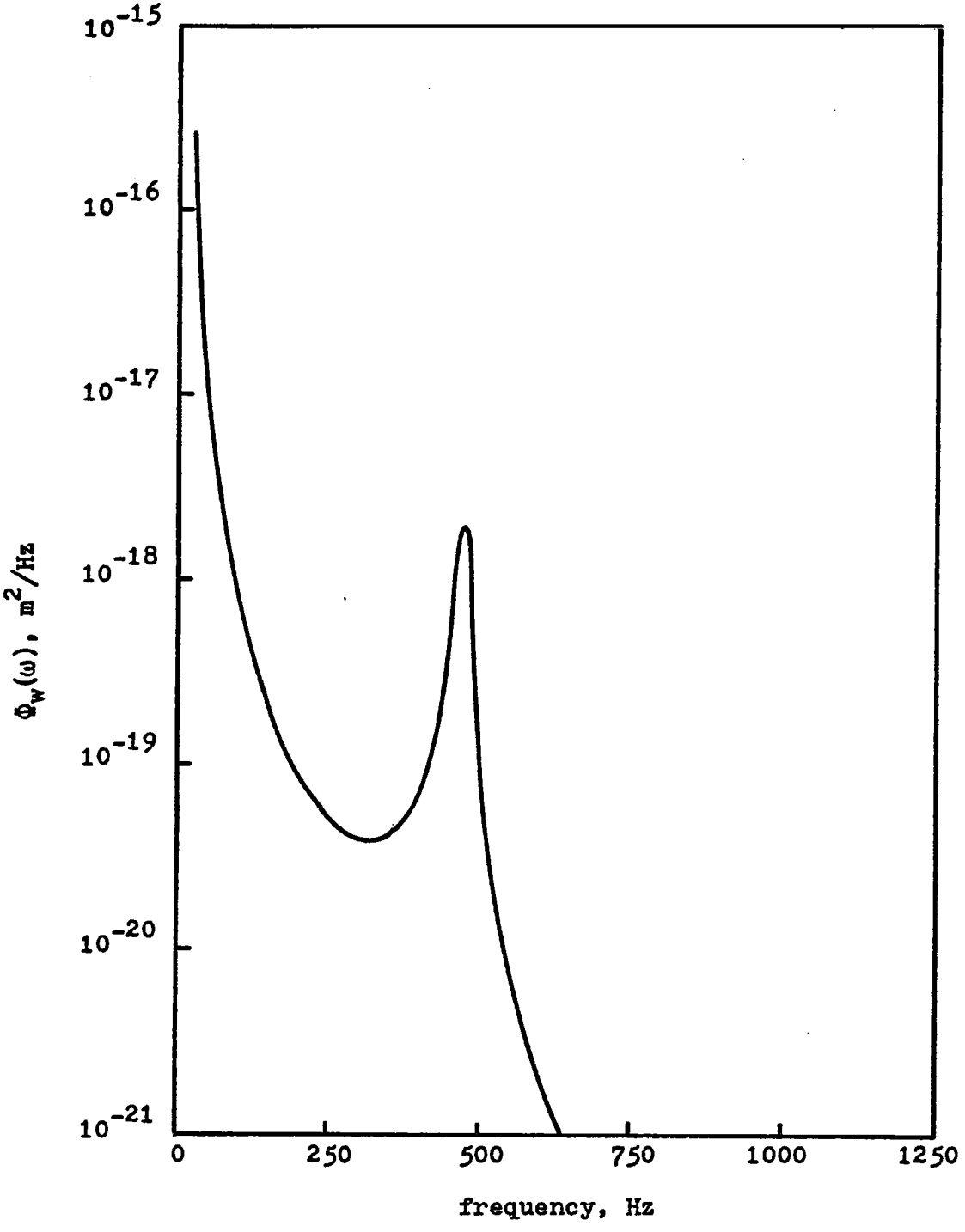

Fig. 3.2 Frequency spectrum of structural displacement under frozen-pattern turbulence excitation

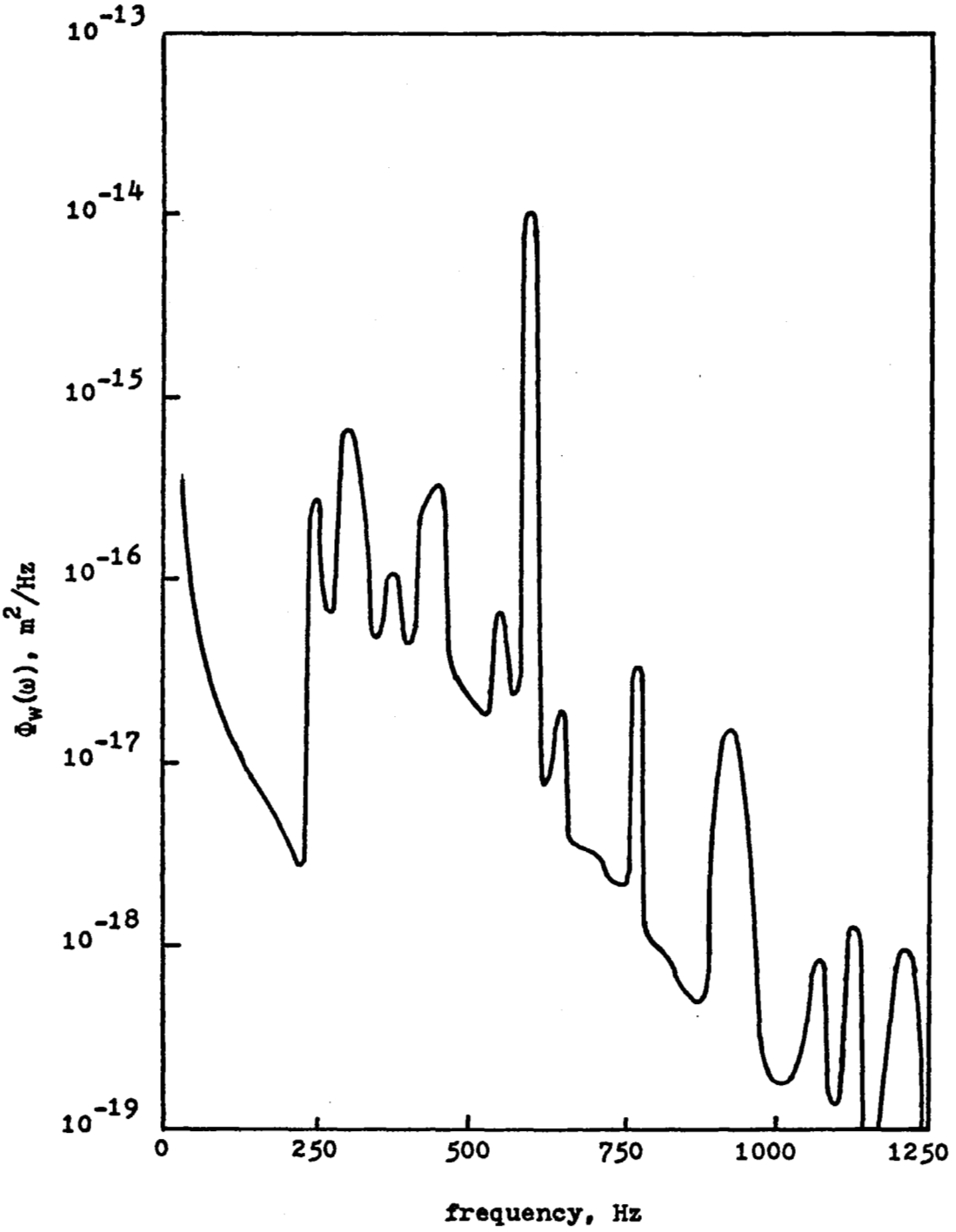

Fig. 3.3 Frequency spectrum of structural displacement under the excitation of the decaying turbulence

frozen-pattern case. Since infinitely many frozen-pattern components are present in the turbulence, the turbulence spectrum has also infinitely many wave-number components at each frequency. Thus, the coincidence (if we may use this terminology in this case) occurs at each frequency. However, the response magnitude may be small if a frozen-pattern component which generates a coincidence wave in the structure has little contribution to the turbulence spectrum at that frequency. Therefore, even the coincidence is present at each frequency, its magnitude varies as the frequency changes and some of them appear as peaks in the response spectrum.

A comparison of Figs. 3.2 and 3.3 shows that the frozen-pattern assumption is unconservative which leads to lower estimates for the structural response and the radiated noise level

3.4 Conclusion

The theory developed in Chapter II has been applied to the simple example of an unsupported beam exposed to boundary-layer excitations. The effect of a cavity and the effect of the free-stream velocity are included in the analysis. The spectral density of the structural displacement response was calculated using the measured turbulence pressure spectrum of a supersonic boundary layer and the result was compared with the solution obtained for the ideal frozen-pattern turbulence. This comparison has shown that

the frozen-pattern assumption leads to considerably lower estimates for the structural response. Thus, we may conclude that the frozen-pattern assumption should not be used in the computation of the structural response spectrum under the excitation of a boundary-layer turbulence pressure.

IV. PERIODICALLY SUPPORTED INFINITE BEAM

4.1 Introduction

In this chapter the turbulence decomposition scheme will be applied to the analysis of an infinite beam supported at uniformly spaced intervals by elastic springs. The elastic supports are simplified versions of reinforcing stringers of an aircraft fuselage. Although an aircraft fuselage is a very complicated multi-panel system its dynamic behavior is similar to that of the periodically supported beam described above. The one-dimensional beam problem, however, is more suitable for fundamental studies since basic concepts can be developed without the burden of mathematical details. Thus, the analysis of the present chapter will be restricted again to one spatial coordinate.

At the first sight the problem of a periodic beam may not appear more difficult than that of any other structure if one accepts the linearity assumption and uses a normal-mode formulation. In practice, however, the normal mode of a periodic beam of many spans cannot be calculated accurately due to close clustering of natural frequencies in frequency bands. The futility of the normal mode approach in dealing with a large number of spans has led to two alternatives: the wave propagation approach (space-harmonic analysis) [17-21] and the transfer matrix approach [10-16]. The two alternative methods are closely related, however. The so-called free wave propagation constants in the first method are the natural

logarithms of the eigenvalues of the basic transfar matrix in the second method [22]. The computational simplicity in both methods is obtained by utilizing the fact that the entire system is composed of identical sub-units in the formulation. The fundamental solution required for the construction of the total structural response is one corresponding to the excitation of a frozen-pattern sinusoid. To obtain this fundamental solution the formulation will follow Mead's wave propagation method, but will take into account the effect of free-stream velocity on the same side of the turbulence excitation and the effect of a cavity on the opposite side of the excitation. As a numerical example, the spectral density of the structural response will be computed and the results will be compared with experimental measurements.

4.2 Wave-Number Response Function of the Infinite Periodic Beam

A sketch of the structural model is shown in Fig. 4.1, surrounded by the same acoustic environment as that assumed in Chapter III.

The governing equation of the beam motion not directly over an elastic support is given by

$$D \frac{\partial^4 w}{\partial x^4} + m \frac{\partial^2 w}{\partial t^2} = p + (p_1 - p_2)_{z=-d} \qquad (4.1)$$

where D denotes the bending rigidity and m is the mass per unit length of the beam. The additional pressure fields denoted by p_1 and p_2 are generated in the fluid media on the

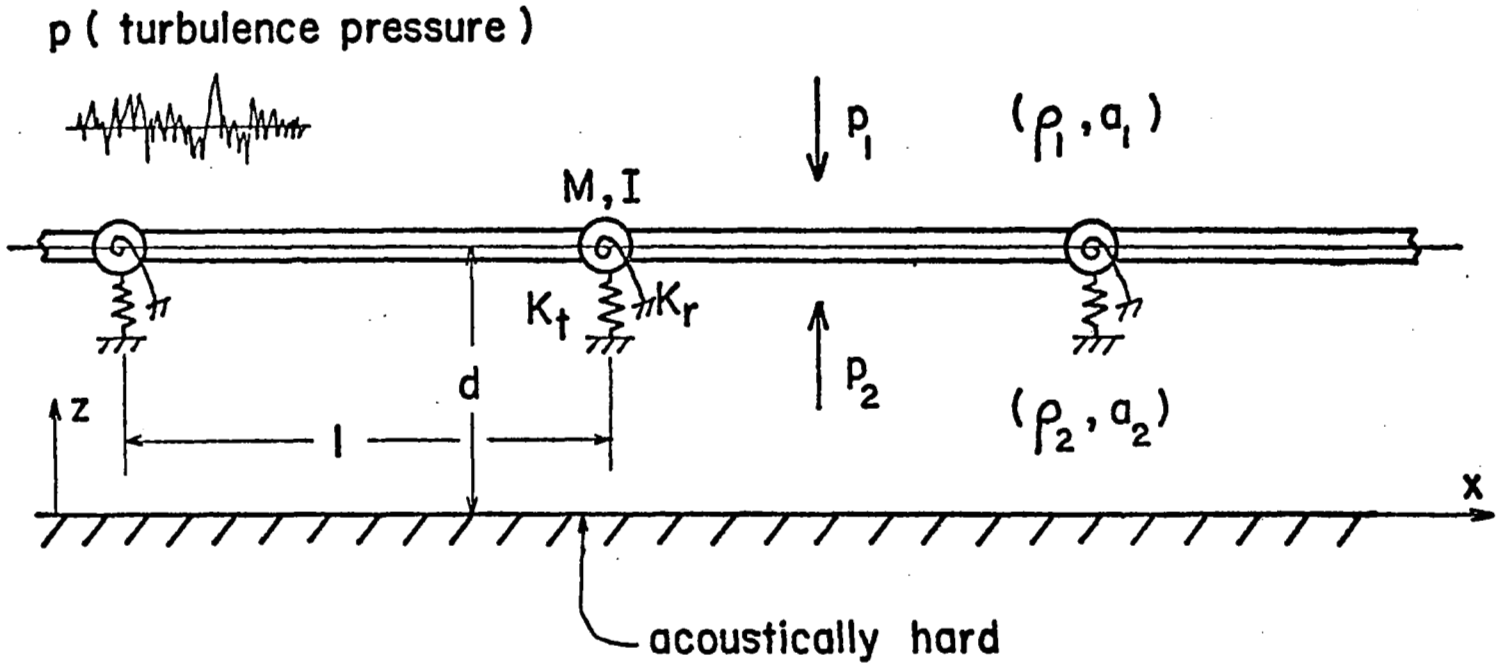

Fig. 4.1 An infinite periodic beam under the excitation of boundary-layer turbulence

upper and lower sides, respectively, due to the beam motion. For the purpose of determining the wave-number response function, H(x,k), the turbulent pressure p should be replaced by exp[i(ωt - kx)] and the structural response w by H(x,k) exp(iωt). Thus, Eq. (4.1) becomes

$$(D\frac{\partial^4 H}{\partial x^4} - m\omega^2 H)\, e^{i\omega t} = e^{i(\omega t - kx)} + (p_1 - p_2)_{z=d} \qquad (4.2)$$

The forcing function exp[i(ωt - kx)] gives every span the same excitation but with a phase-lag $\mu_0 = k\ell$ from one span to the next. In this sense μ_0 may be considered as the imposed phase-lag of the excitation. To satisfy the spatial periodicity in the structural response Mead suggested the following series form [18]:

$$H(x,k) = \sum_{n=-\infty}^{\infty} A_n \exp(-\frac{i\mu_n x}{\ell}) \qquad (4.3)$$

where

$$\mu_n = \mu_0 + 2n\pi = k\ell + 2n\pi \qquad (4.4)$$

Without the elastic supports the wave-number response function would be just the one term associated with the forcing phase-lag μ_0. The elastic supports give rise to multiple reflections, thereby admitting other μ_n values.

For the induced additional pressure p_1, we apply the same assumption used in the preceding chapter. Then p_1 is governed by the equation

$$\left(\frac{\partial}{\partial t} + U_\infty \frac{\partial}{\partial x}\right)^2 p_1 - a_1^2 \left(\frac{\partial^2}{\partial x^2} + \frac{\partial^2}{\partial z^2}\right) p_1 = 0 \qquad (4.5)$$

and subject to the conditions that p_1 can propagate only in the region $z > d$, and that

$$\left(\frac{\partial p_1}{\partial z}\right)_{z=d} = \rho_1 \left(i\omega + U_\infty \frac{\partial}{\partial x}\right)^2 H\, e^{i\omega t} \qquad (4.6)$$

The solution for p_1 corresponding to each component in the wave-number response function $A_n \exp(-i\mu_n x/\ell)$ is known. The total p_1 can then be obtained by superposition. This pressure, when evaluated at $z = d$, is given by [31]

$$p_1\Big|_{z=d} = -i\rho_1 a_1 \sum_{n=-\infty}^{\infty} A_n \frac{(u_n - U_\infty)^2}{(\ell/\mu_n)\left[(u_n - U_\infty)^2 - a_1^2\right]^{\frac{1}{2}}} e^{i(\omega t - \mu_n x/\ell)} \qquad (4.7)$$

where

$$u_n = \frac{\omega \ell}{\mu_n} \qquad (4.8)$$

The same comments which were made previously relative to Eq. (3.4) apply in this case to each term in Eq. (4.7). Each component now has a different propagation speed u_n instead of the one propagation speed ω/k in Eq. (3.4). For emphasis and clarity these comments are restated as follows: (1) u_n is the speed at which the component structural motion $A_n \exp[i(\omega t - \mu_n x/\ell)]$ is propagated along the beam. (2) A component structural motion generates no pressure in the adjacent fluid medium if it is propagated at the same velocity as that of the

fluid medium (the case of $u_n = U_\infty$). (3) Theoretically, the generated pressure attains an infinite amplitude when the propagation velocity of the structural motion relative to the medium is equal to the speed of sound (the case of $|u_n - U_\infty| = a_1$, the shock wave effect). (4) When this relative velocity is less than the speed of sound; i.e., $|u_n - U_\infty| < a_1$, the generated pressure should provide additional inertia for the structural motion (the apparent mass effect); therefore, a negative imaginary value should be given to the square-root $[(u_n - U_\infty)^2 - a_1^2]^{\frac{1}{2}}$ in the calculation.

The induced pressure p_2 in the fluid medium $0 \leq z < d$ is governed by

$$\frac{\partial^2 p_2}{\partial t^2} - a_2^2 \left(\frac{\partial^2}{\partial x^2} + \frac{\partial^2}{\partial z^2}\right) p_2 = 0 \tag{4.9}$$

and subject to the conditions

$$\frac{\partial p_2}{\partial z} = 0 \quad \text{at } z = 0 \tag{4.10}$$

$$\frac{\partial p_2}{\partial z} = -\rho_2 \omega^2 H e^{i\omega t} \quad \text{at } z = d \tag{4.11}$$

The solution for p_2, when evaluated at $z = d$, is given by

$$p_2\big|_{z=d} = \rho_2 \omega^2 \sum_{n=-\infty}^{\infty} A_n \frac{\cot(\gamma_n d)}{\gamma_n} e^{i(\omega t - \mu_n x/\ell)} \tag{4.12}$$

where

$$\gamma_n^2 = \left(\frac{\omega}{a_2}\right)^2 - \left(\frac{\mu_n}{\ell}\right)^2 \tag{4.13}$$

For a small d and a positive γ_n^2, the n-th component of this transmitted pressure p_2 gives rise to additional stiffness on the structural motion and for certain ranges of d value it can become an added mass to the system. When γ_n^2 is negative, γ_n becomes imaginary in which case

$$\frac{\cot(\gamma_n d)}{\gamma_n} = -\frac{\coth|\gamma_n d|}{|\gamma_n|} \tag{4.14}$$

and the component always contributes to the system inertia regardless of the value of d.

Equations (4.3), (4.7) and (4.12) can now be substituted into Eq. (4.2) to obtain

$$\sum_{n=-\infty}^{\infty} A_n \varphi(n) \exp(-i\mu_n x/\ell) = \exp(-i\mu_0 x/\ell) \tag{4.15}$$

where

$$\varphi(n) = D\left(\frac{\mu_n}{\ell}\right)^4 - m\omega^2 + i\rho_1 a_1 \frac{(u_n - U_\infty)^2}{(\ell/\mu_n)[(u_n - U_\infty)^2 - a_1^2]^{\frac{1}{2}}} + \rho_2\omega^2 \frac{\cot(\gamma_n d)}{\gamma_n} \tag{4.16}$$

To determine the amplitude A_n we follow Mead's procedure [19] and calculate the virtual work done by the external forces acting on the structure and by the internal forces in the structure through a virtual displacement

$$\delta A_j \, e^{-i(\omega t - \mu_j x/\ell)}$$

Excluding the elastic supports, the virtual work done within one span of the beam is

$$\delta W_b = \delta A_j \Big[\sum_{n=-\infty}^{\infty} A_n \varphi(n) \int_0^{\ell} e^{-i\mu_n x/\ell} \; e^{i\mu_j x/\ell} \; dx - \int_0^{\ell} e^{-i\mu_0 x/\ell} \; e^{i\mu_j x/\ell} \; dx \Big] \tag{4.17}$$

The elastic supports are characterized by a translational spring constant K_t, a translational inertia M, a torsional spring constant K_r, and a torsional inertia I. Thus the virtual work contributed by each elastic spring is

$$\begin{aligned} \delta W_e &= \delta W_t + \delta W_r \\ &= (K_t - M\omega^2) \, \delta A_j \sum_{n=-\infty}^{\infty} A_n + (k_r - I\omega^2) \\ &\quad \left(\frac{\mu_j}{\ell}\right) \delta A_j \sum_{n=-\infty}^{\infty} \left(\frac{\mu_n}{\ell}\right) A_n \end{aligned} \tag{4.18}$$

Since the structural motion is spatially periodic the virtual work done throughout the entire structure is proportional to that of a periodic unit. Therefore, the principle of virtual work can be stated for a periodic unit as follows:

$$\delta W_b + \delta W_t + \delta W_r = 0 \tag{4.19}$$

which leads to the simultaneous algebraic equations:

$$A_j \varphi(j) + \frac{K_t - M\omega^2}{\ell} \sum_{n=-\infty}^{\infty} A_n + \frac{K_r - I\omega^2}{\ell} \frac{\mu_j}{\ell} \sum_{n=-\infty}^{\infty} \frac{\mu_n}{\ell} A_n$$

$$= \begin{cases} 1, & \text{if } j = 0 \\ 0, & \text{if } j \neq 0 \end{cases} \tag{4.20}$$

In actual computations the number of simultaneous equations must be truncated. One can, for example, solve a system of $2N + 1$ equations corresponding to $-N \leq j \leq N$. The choice of N must be such that the truncated version of the wave-number response, Eq. (4.3), do not change appreciably by further increase of the number of terms used in the computation.

Equations (4.20) are derived for finite $K_t - M\omega^2$ and finite $K_r - I\omega^2$, and these equations cannot be reduced to those for supports rigid in translation or rotation. For example, if the supports are rigid in translation then K_t becomes infinitely large, but the summation of all the A_n must be zero since the deflection at each support is zero, and the product of these two becomes indefinite. To deal with this case, substitute

$$A_0 = - \sum_{\substack{n=-\infty \\ n\neq 0}}^{\infty} A_n \tag{4.21}$$

into Eq. (4.3) to obtain

$$H(x,k) = \sum_{\substack{n=-\infty \\ n\neq 0}}^{\infty} A_n \left(e^{-i\mu_n x/\ell} - e^{-i\mu_0 x/\ell}\right) \tag{4.22}$$

Correspondingly, virtual displacements are chosen in the form of

$$\delta A_j \left(e^{i\mu_j x/\ell} - e^{i\mu_0 x/\ell}\right) e^{-i\omega t}$$

Then, instead of Eq. (4.20), one obtains from a similar derivation

$$A_j\varphi(j) + \varphi(0)\sum_{\substack{n=-\infty \\ n\neq 0}}^{\infty} A_n + \frac{K_r - I\omega^2}{\ell}\frac{\mu_j - \mu_0}{\ell}\sum_{\substack{n=-\infty \\ n\neq 0}}^{\infty}\frac{\mu_n - \mu_0}{\ell}A_n$$

$$= -1, \quad j \neq 0 \tag{4.23}$$

It is interesting to note that if the supports are rigid in translation but without constraints in rotation (the case of hinge supports) the equations for A_j can be decoupled. For such a case, Eq. (4.23) reduces to

$$A_j\varphi(j) + \varphi(0)\sum_{\substack{n=-\infty \\ n\neq 0}}^{\infty} A_n = -1, \quad j \neq 0 \tag{4.24}$$

Eq. (4.24) shows that the product $A_j\varphi(j)$ is independent of j; i.e.,

$$A_1\varphi(1) = A_2\varphi(2) = \cdots \tag{4.25}$$

Thus, substituting

$$A_n = A_j\varphi(j)/\varphi(n) \tag{4.26}$$

into Eq. (4.24), one obtains equations involving only one unknown:

$$A_j\varphi(j)\varphi(0)\sum_{n=-\infty}^{\infty}\frac{1}{\varphi(n)} = -1 \tag{4.27}$$

which is solved readily to give

$$A_j = -\left[\varphi(j)\varphi(0)\sum_{n=-\infty}^{\infty}\frac{1}{\varphi(n)}\right]^{-1} \tag{4.28}$$

Uncoupled solutions such as Eq. (4.28) are not restricted to the case of hinge supports. In fact, if one of the two infinite sums in Eq. (4.20) can be dropped, a substitution of the type of Eq. (4.26) is possible which is the key for reducing Eq. (4.24) to Eq. (4.27) containing only one A_j in each equation. This is the case when either $K_t - M\omega^2 = 0$ or $K_r - I\omega^2 = 0$; i.e., when the elastic supports offer no translational constraint or no rotational constraint.

If the rotational constraint is infinite, one again cannot obtain a reduced equation from Eq. (4.20) which is valid only for finite support constraints. To derive a reduced equation one must use the zero slope condition at the supports

$$\sum_{n=-\infty}^{\infty}\mu_n A_n = 0 \tag{4.29}$$

The remaining procedure is very similar to that leading to Eq. (4.24)

Now, we are ready to compute the spectral density of the structural response. Once A_j are determined by either one of Eqs. (4.20), (4.23) or (4.28) depending on the problem, they can be substituted into Eq. (4.3) to obtain the wave-number response function, H. Further substitution of this H function into Eq. (2.36) along with the statistical properties of the turbulence pressure gives the cross-spectral

density of the structural displacement response.

4.3 Numerical Example

To illustrate the application of the present theory, the spectral densities of the acceleration response at a mid-span location (i.e., $x_1 = x_2 = \ell/2$) have been computed based on the following physical data:

properties of the beam:

D (bending rigidity) = 3.935×10^4 N-m^2

ℓ (span-length) = 0.508 m

m (mass per unit length) = 9.746 Kg/m

properties of the surrounding fluid media:

$\rho_1 = \rho_2 = \rho$ (density) = 0.11015 Kg/m^3

$a_1 = a_2 = a$ (speed of sound) = 261.6 m/sec

U_∞ (free-stream velocity on upper side of beam) = 575.6 m/sec

d (cavity depth) = 0.1178 m

properties of the turbulent pressure [28]:

$\overline{\Phi}_p(0,\omega)$ = spectral density = $\frac{1}{2}\frac{\delta}{U_\infty}\sum_{n=1}^{4} A_n e^{-K_n(|\omega|\delta/U_\infty)}$

$\psi(\xi)$ = decay factor = $\exp(-\frac{|\xi|}{\alpha\delta})$

U_c (characteristic convection velocity of the turbulence) = 0.75 U_∞

δ (boundary-layer thickness) = 0.279 m

$\alpha = 3$

$A_1 = 4.4 \times 10^{-2}$ $\quad K_1 = 5.78 \times 10^{-2}$

$A_2 = 7.5 \times 10^{-2}$ $\quad K_2 = 2.43 \times 10^{-1}$

$A_3 = -9.3 \times 10^{-2}$ $\quad K_3 = 1.12$

$A_4 = -2.5 \times 10^{-2}$ $\quad K_4 = 11.57$

Except for the additional information about the span length ℓ the above physical data are the same as those used previously for the unsupported beam, and they were taken from a recent experiment on a multi-panel system [28]. The structural specimen used in this experiment was actually a two-dimensional panel array as shown in Fig. 4.2. Therefore, some data have been converted to their one-dimensional equivalents. For example, the bending rigidity D of the beam was the average value for the skin and the reinforcing stringers over a unit width, and the specific mass m was obtained similarly. Although the actual structural specimen had only seven spans and the two end-spans were somewhat shorter, it was felt that the theory of an infinite periodic beam on evenly spaced supports should give a reasonable result for the response spectrum at the center of the middle span where accelerometer A20 was located (referred to Fig. 4.2), and where the effects of the end spans were least important. The translational constraints provided by the supporting frames were sufficiently strong to justify taking the translational spring constant K_t of the supports to be infinite (i.e., the deflections at the supports were assumed to be zero). For the rotational constraints we selected $K_r = 60$ N-m/rad and $I = 3.3 \times 10^{-4}$ Kg-m^2. These are the one-dimensional equivalents of the torsional

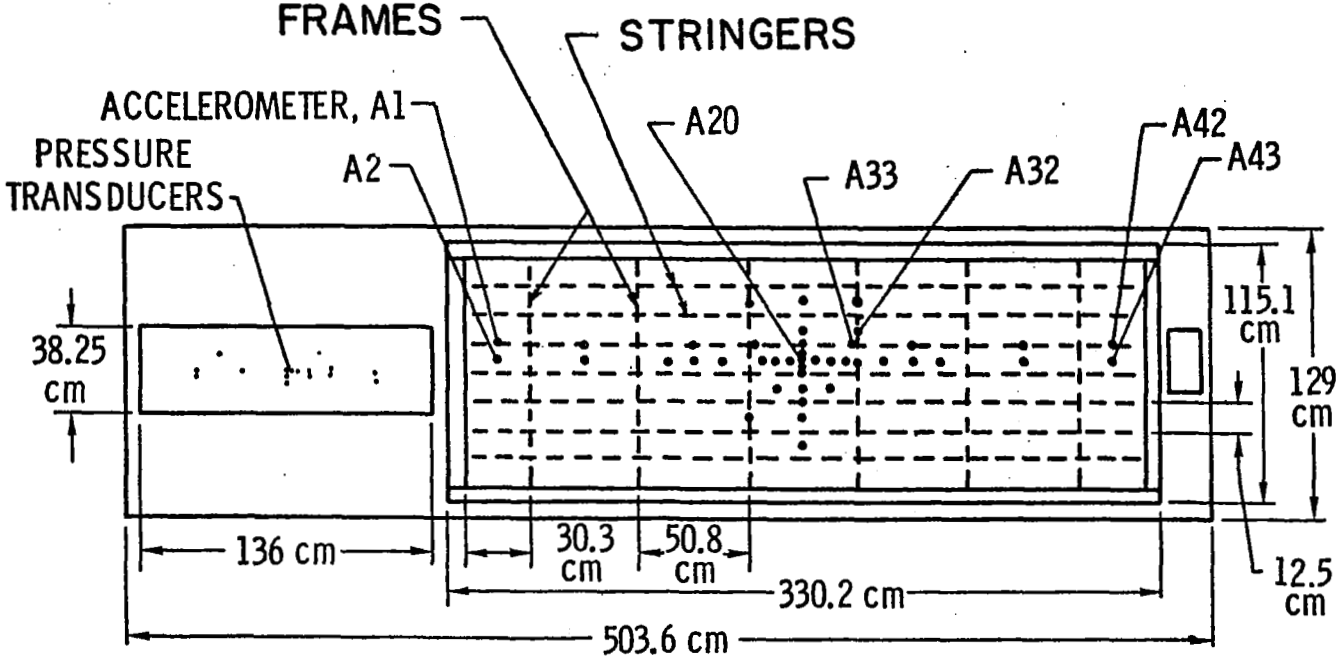

Fig. 4.2 The experimental set-up

constraints of the frames if the torsional mode of each frame is a half-sine curve.

In order to minimize the computer cost, the computation was carried out only to 3000 Hz and at the intervals of every 50 Hz. The resolution of the computed spectrum was compromised somewhat by the use of coarse intervals, but our main objective was to find the general trend which could be revealed by the values at 50 Hz intervals.

In Fig. 4.3 the computed spectrum is shown along with the experimental spectrum. As it is customary, the experimental spectrum is one-sided (restricted to the positive frequency domain); therefore, the theoretical spectrum has been converted by multiplying the computed two-sided values by two. It also should be noted that the experimental results were obtained using a filter of 1 Hz bandwidth. This accounts for its much more rugged appearance than the theoretical one computed at much larger intervals of 50 Hz. Furthermore, experimentally obtained signals may contain noise other than the structural response. Although the theoretical and the experimental curves show the same general trend, the former is lower than the latter throughout the entire frequency range investigated. This is to be expected since the theoretical curve represents the average between the panel response and the stringer response, whereas the experimental curve shows the panel response alone.

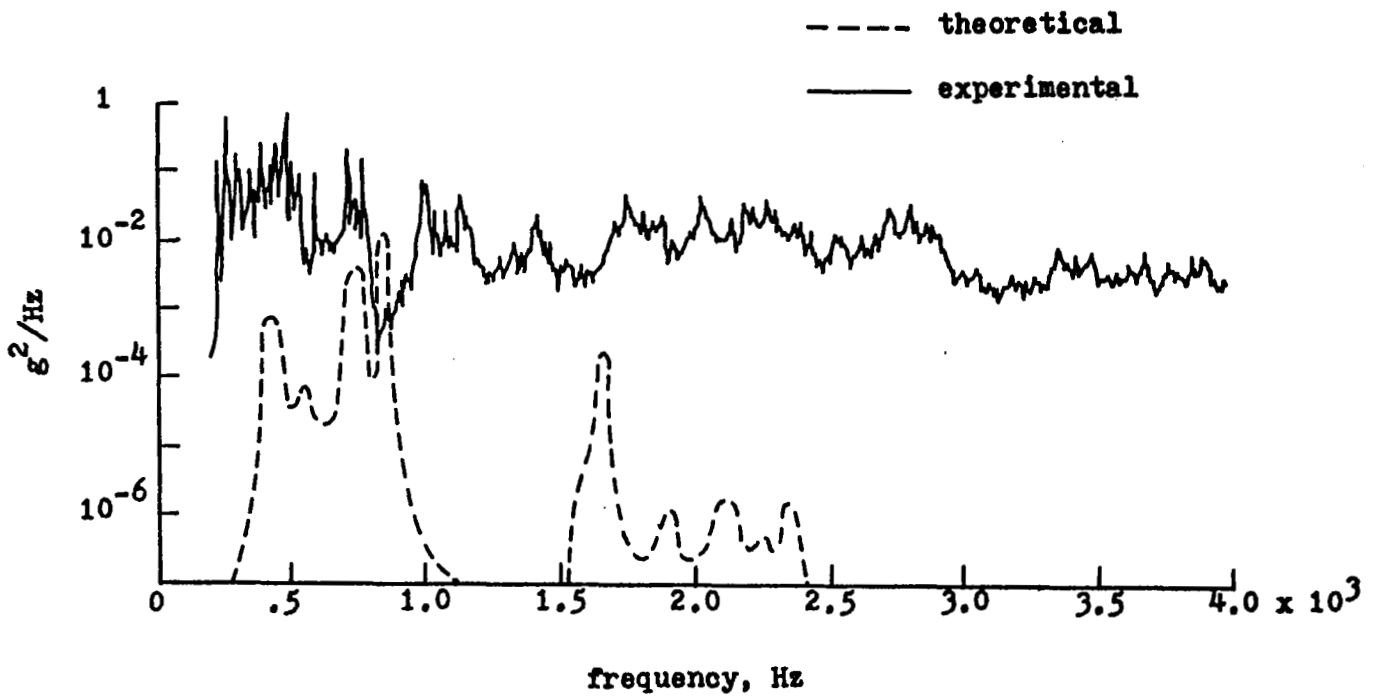

Fig. 4.3 Acceleration spectra of structural response

4.4 Conclusion

The case of fluid-loaded infinite periodic beam, considered in this chapter, is one of the very few where a mathematically exact solution for the wave-number response function, H, can be obtained. If the beam is finite in length then the method of transfer matrix may be more preferable; however, the effect of fluid loading cannot be accounted for exactly (in the mathematical sense) at the present time.

Further extensions to the two-dimensional case of panel systems are obvious. If only one row of panels is considered, and if the two parallel edges of the panel row are assumed to be simply supported, then separation of spatial variables is possible in expressing the structural response. This is the well-known Levy's type solution for plate problems. With small modifications, the solution for the one-dimensional beam case can be changed to suit such a panel row problem. When more than one row of panels are included in the structural model the separation of spatial variables in the structural motion is no longer mathematically exact, but a separable form can still be used as an approximation. Although new concepts are not required in treating such two-dimensional problems, the machine computation time can become extremely excessive and burdensome to small research budgets.

V. MEMBRANE WITH RANDOM TENSION

5.1 Introduction

The unsupported infinite beam and the periodically supported infinite beam discussed in the preceding chapters are idealized models. However, actual structures cannot be constructed in ideal manners. The material properties vary randomly throughout the entire structure and manufacturing errors always exist in size and shape such as the span length and the cross-section of a beam, the pre-tension in a membrane, etc. It has been shown by Lin and Yang [33-35] that in the case of a periodic beam the randomness in the structure properties causes appreciable variations in the structural response from the ideal model results. In this chapter, the structural response of a membrane to the subsonic boundary-layer turbulence will be investigated. The pre-tension in the membrane will be treated as a random process in space, and the membrane is surrounded by an acoustic environment similar to that in the preceding chapters.

5.2 Wave-Number Response Function of Membrane

The structural model chosen for the present study is a membrane which is infinitely long in the x-direction and is fixed along y = 0 and y = b as shown in Fig. 5.1. This membrane is backed on the lower side by a cavity of depth d which is filled with an initially quiescent fluid of density ρ_2 and sound speed a_2. On the upper side the membrane is

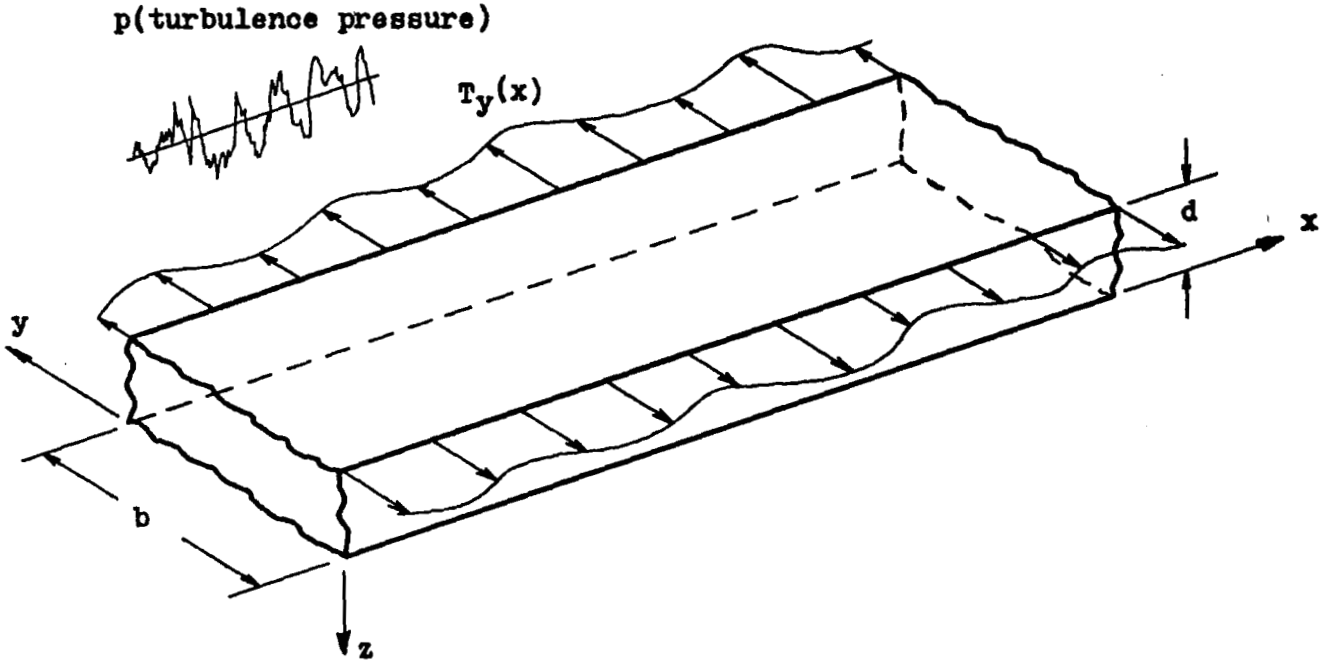

Fig. 5.1 An infinite membrane with random tension under the excitation of boundary-layer turbulence

exposed to the excitation of a subsonic boundary-layer turbulent pressure p. The fluid on the upper side of the membrane which carries the turbulence has a free-stream velocity U_∞, density ρ_1 and sound speed a_1. The design pre-tension in the membrane is T_0; however, it will be assumed that this uniform tension can only be achieved in the x-direction but in the manufacturing process a small random variation $\epsilon f(x)$ has developed in the y-direction where $\epsilon \ll 1$.

As the membrane responds to the excitation its motion will generate additional pressures in the fluid media on the upper and the lower sides. Denoting such pressures by p_1 and p_2, respectively, the governing equation of the membrane is given by

$$m\frac{\partial^2 w}{\partial t^2} + \gamma\frac{\partial w}{\partial t} - T_0\frac{\partial^2 w}{\partial x^2} - [T_0 + \epsilon f(x)]\frac{\partial^2 w}{\partial y^2}$$

$$= p + (p_1 - p_2)_{z=-d} \qquad (5.1)$$

where m is the mass of the membrane per unit area, γ is the viscous damping coefficient.

As discussed in Chapter II, the turbulent pressure p should be replaced by $\exp[i(\omega t - kx)]\,\delta(y - y')$ and the structural response w by $H(x,k,y,y',\omega)\exp(i\omega t)$ for the purpose of determining the wave-number response function $H(x,k,y,y',\omega)$. Thus, Eq. (5.1) becomes

$$\{-m\omega^2 H + i\gamma\omega H - T_0\frac{\partial^2 H}{\partial x^2} - [T_0 + \epsilon f(x)]\frac{\partial^2 H}{\partial y^2}\}\, e^{i\omega t}$$

$$= e^{i(\omega t - kx)} \delta(y - y') + (p_1 - p_2)_{z=-d} \qquad (5.2)$$

The boundary conditions for the wave-number response function H are

$$H(x,k,y,y',\omega) = 0 \quad \text{at } y = 0,\ b \qquad (5.3)$$

These boundary conditions are automatically satisfied if H is expressed in a Levy type series

$$H(x,k,y,y',\omega) = \sum_{n=1}^{\infty} \sin \frac{n\pi y}{b} \int_{-\infty}^{\infty} A_n(\mu,k,y',\omega)\ e^{-i\mu x}\, d\mu \qquad (5.4)$$

In the sequel the symbol $A_n(\mu)$ will be used in lieu of $A_n(\mu, k,y',\omega)$ for compactness.

For the determination of the radiation pressure p_1, we use the usual approximation that it can be calculated without regard to the presence of the turbulence. Under this condition, the radiated pressure p_1 is governed by

$$\left(\frac{\partial}{\partial t} + U_\infty \frac{\partial}{\partial x}\right)^2 p_1 - a_1^2 \left(\frac{\partial^2}{\partial x^2} + \frac{\partial^2}{\partial y^2} + \frac{\partial^2}{\partial z^2}\right) p_1 = 0 \qquad (5.5)$$

with the boundary condition

$$\left.\frac{\partial p_1}{\partial z}\right|_{z=-d} = -\rho_1 \left(\frac{\partial}{\partial t} + U_\infty \frac{\partial}{\partial x}\right)^2 H\, e^{i\omega t} \qquad (5.6)$$

The exact solution for p_1 is unknown but in close proximity to the membrane p_1 can be approximated by the expression

$$p_1 = e^{i\omega t} \sum_{n=1}^{\infty} \sin \frac{n\pi y}{b} \int_{-\infty}^{\infty} g_n(z,\mu)\, e^{-i\mu x}\, d\mu \qquad (5.7)$$

Substituting Eq. (5.7) into Eq. (5.5), multiplying both sides of the equation with $\sin(n'\pi y/b)\, \exp(i\mu' x)$, and integrating over $-\infty < x < \infty$ and $0 < y < b$, one obtains

$$g_n''(z,\mu) - k_n^2(\mu)\, g_n(z,\mu) = 0 \qquad (5.8)$$

where

$$k_n^2(\mu) = \mu^2 + \left(\frac{n\pi}{b}\right)^2 - \left(\frac{\omega}{a_1} - \frac{U_\infty}{a_1}\mu\right)^2 \qquad (5.9)$$

Equation (5.8) is solved, with the condition that p_1 only propagates in the negative z-domain, to give

$$g_n(z,\mu) = C_n(\mu)\, \exp[k_n(\mu) z] \qquad (5.10)$$

Substituting Eqs. (5.4), (5.7) and (5.10) into Eq.(5.6), and using the orthogonality properties, we have

$$C_n(\mu) = \rho_1 \frac{(\omega - U_\infty \mu)^2}{k_n(\mu)}\, e^{k_n(\mu) d}\, A_n(\mu) \qquad (5.11)$$

Therefore, the radiation pressure p_1, when evaluated at $z = -d$, is

$$p_1\Big|_{z=-d} = \rho_1\, e^{i\omega t} \sum_{n=1}^{\infty} \sin \frac{n\pi y}{b} \int_{-\infty}^{\infty} \frac{(\omega - U_\infty \mu)^2}{k_n(\mu)}\, A_n(\mu)\, e^{-i\mu x}\, d\mu \qquad (5.12)$$

The transmitted pressure p_2 is governed by the Helmholtz equation

$$\frac{\partial^2 p_2}{\partial t^2} - a_2^2 \left(\frac{\partial^2}{\partial x^2} + \frac{\partial^2}{\partial y^2} + \frac{\partial^2}{\partial z^2}\right) p_2 = 0 \tag{5.13}$$

and is subject to the boundary conditions

$$\frac{\partial p_2}{\partial z} = 0 \quad \text{at } z = 0 \tag{5.14}$$

$$\frac{\partial p_2}{\partial z} = \rho_2 \omega^2 H e^{i\omega t} \quad \text{at } z = -d \tag{5.15}$$

$$\frac{\partial p_2}{\partial y} = 0 \quad \text{at } y = 0, b \tag{5.16}$$

The conditions (5.14) and (5.16) corresponds to the ideal case where the bottom and side walls of the cavity are acoustically hard. The solution of this system is given by

$$p_2\Big|_{z=-d} = \rho_2 \omega^2 e^{i\omega t} \sum_{\substack{n=1 \\ n+r=\text{odd}}}^{\infty} \sum_{r=0}^{\infty} \cos\frac{r\pi y}{b} \frac{4}{\pi g(r)} \frac{n}{n^2 - r^2} \int_{-\infty}^{\infty} \frac{\cot \bar{k}_r(\mu) d}{\bar{k}_r(\mu)} A_n(\mu) e^{-i\mu x} d\mu \tag{5.17}$$

where

$$\bar{k}_r^2(\mu) = \left(\frac{\omega}{a_2}\right)^2 - \mu^2 - \left(\frac{r\pi}{b}\right)^2 \tag{5.18}$$

$$g(r) = \begin{cases} 2, & r = 0 \\ 1, & r \neq 0 \end{cases} \tag{5.19}$$

Substituting Eqs. (5.4), (5.12) and (5.17) into Eq. (5.2), we

have

$$\varphi_n(\mu)A_n(\mu) + \sum_{\ell=1}^{\infty} A_\ell(\mu)\psi_{n\ell}(\mu)$$

$$+ \epsilon\left(\frac{n\pi}{b}\right)^2 \int_{-\infty}^{\infty} A_n(\lambda)\left[\frac{1}{2\pi}\int_{-\infty}^{\infty} f(x)\, e^{i(\mu - \lambda)x}\, dx\right] d\lambda$$

$$= \left(\frac{2}{b}\right)\delta(\mu - k)\sin\frac{n\pi y'}{b} \qquad (5.20)$$

where

$$\varphi_n(\mu) = -m\omega^2 + i\gamma\omega + T_0\left(\frac{n\pi}{b}\right)^2 + T_0\mu^2 - \rho_1\frac{(\omega - U_\infty\mu)^2}{k_n(\mu)} \qquad (5.21)$$

$$\psi_{n\ell}(\mu) = \rho_2\omega^2 \sum_{\substack{r=0 \\ n+r=\text{odd} \\ \ell+r=\text{odd}}}^{\infty} \frac{16}{\pi^2 g(r)}\,\frac{\cot \bar{k}_r(\mu)d}{\bar{k}_r(\mu)}\,\frac{n}{n^2 - r^2}\,\frac{\ell}{\ell^2 - r^2} \qquad (5.22)$$

In the present study Eq. (5.20) will be solved for the following two cases:

$$\text{case I} \quad ; \quad f(x) = 0$$

$$\text{case II} \quad ; \quad f(x) = \sum_{j=-M}^{M} X_j \exp(ij\nu x), \qquad X_0 = 0$$

Case I corresponds to the ideal uniform tension problem; i.e., the tension in the membrane is equal to the constant T_0 in all directions. Case II represents the case where random variation of tension in the membrane can be expressed as a superposition of sinusoidal variations. The fundamental wave number ν will be assumed to be deterministic and the complex amplitudes, X_j, random variables.

CASE I ; $f(x) = 0$

In this case Eq. (5.20) reduces to

$$\varphi_n(\mu)\, A_n(\mu) + \sum_{\ell=1}^{\infty} A_\ell(\mu)\, \psi_{n\ell}(\mu) = \left(\frac{2}{b}\right) \sin\frac{n\pi y'}{b}\, \delta(\mu - k) \tag{5.23}$$

which is an infinite set of simultaneous equations in A_n. In actual computations the number of simultaneous equations must be truncated. One can solve a system of N equations corresponding to $1 \leq n \leq N$. The choice of N must be such that the truncated version of the structural response, (5.4), is sufficiently accurate and it does not change appreciably by further increase of the number of terms. After truncating the number of simultaneous equations, Eq. (5.23) can be written in a matrix form

$$[K_1(\mu)]\, \{A(\mu)\} = \{P\}\, \delta(\mu - k) \tag{5.24}$$

where the elements of the matrix K_1 and the vector P are

$$K_{1_{n\ell}}(\mu) = \varphi_n(\mu)\, \delta_{n\ell} + \psi_{n\ell}(\mu) \tag{5.25}$$

$$P_n = \left(\frac{2}{b}\right) \sin\frac{n\pi y'}{b} \tag{5.26}$$

and $\delta_{n\ell}$ is a Kronecker delta having the property:

$$\delta_{n\ell} = \begin{cases} 1, & n = \ell \\ 0, & n \neq \ell \end{cases} \tag{5.27}$$

The solution of Eq. (5.24) is

$$\{A(\mu)\} = [K_1(\mu)]^{-1} \{P\} \delta(\mu - k) \tag{5.28}$$

Substitution of Eq. (5.28) into Eq. (5.4) yields

$$H(x,k,y,y',\omega) = \sum_{n=1}^{N} R_n \sin \frac{n\pi y}{b} \tag{5.29}$$

where R_n is the n-th element of the vector R which is defined as

$$\{R\} = [K_1(k)]^{-1} \{P\} e^{-ikx} \tag{5.30}$$

CASE II ; $f(x) = \sum_{j=-M}^{M} X_j \exp(ij\nu x)$, $X_0 = 0$

In this case Eq. (5.20) reduces to

$$\varphi_n(\mu) A_n(\mu) + \sum_{\ell=1}^{N} A_\ell(\mu) \psi_{n\ell}(\mu) + \epsilon(\frac{n\pi}{b})^2$$

$$\sum_{j=-M}^{M} X_j A_n(\mu + j\nu) = (\frac{2}{b}) \sin \frac{n\pi y'}{b} \delta(\mu - k) \tag{5.31}$$

where the number of the simultaneous equations has been truncated to N. In a matrix form

$$[K_1(\mu)] \{A(\mu)\} + \epsilon[K_2] \sum_{j=-M}^{M} X_j \{A(\mu + j\nu)\}$$

$$= \{P\} \delta(\mu - k) \tag{5.32}$$

where the elements of the matrix K_2 are

$$K_{2_{n\ell}} = (\frac{n\pi}{b})^2 \delta_{n\ell} \tag{5.33}$$

which show that the matrix K_2 is a diagonal matrix. To solve Eq. (5.32) $[A(\mu)]$ is expanded in a series, keeping in mind that ϵ is a small quantity,

$$\{A(\mu)\} = \{^0A(\mu)\} + \epsilon\{^1A(\mu)\} + \epsilon^2\{^2A(\mu)\} + \cdots \quad (5.34)$$

Substituting Eq. (5.34) into Eq. (5.32), and grouping terms of the first and second powers of ϵ, one obtains

$$[K_1(\mu)]\ \{^0A(\mu)\} = \{P\}\ \delta(\mu - k) \quad (5.35)$$

$$[K_1(\mu)]\ \{^1A(\mu)\} = -\ [K_2]\ \sum_{j=-M}^{M} X_j\{^0A(\mu + j\nu)\} \quad (5.36)$$

$$[K_1(\mu)]\ \{^2A(\mu)\} = -\ [K_2]\ \sum_{j=-M}^{M} X_j\{^1A(\mu + j\nu)\} \quad (5.37)$$

Eq. (5.35) is solved to give

$$\{^0A(\mu)\} = [K_1(\mu)]^{-1}\ \{P\}\ \delta(\mu - k) \quad (5.38)$$

Substituting Eq. (5.38) into Eq. (5.36), we have

$$\{^1A(\mu)\} = -\ [K_1(\mu)]^{-1}[K_2]\ \sum_{j=-M}^{M} X_j[K_1(\mu + j\nu)]^{-1}$$

$$\{P\}\ \delta(\mu + j\nu - k) \quad (5.39)$$

Likewise,

$$\{^2A(\mu)\} = [K_1(\mu)]^{-1}[K_2]\ \sum_{j=-M}^{M}\ \sum_{q=-M}^{M} X_j\ X_q^*$$

$$[K_1(\mu - q\nu)]^{-1}[K_2]\ [K_1(\mu + j\nu - q\nu)]^{-1}$$

$$\{P\}\ \delta(\mu + j\nu - q\nu - k)$$

Thus, to the order of ϵ^2, we have

$$H(x,k,y,y',\omega) = \sum_{n=1}^{N} \sin\frac{n\pi y}{b}\left[R_n + \epsilon \sum_{j=-M}^{M} X_j F_n^j + \epsilon^2 \sum_{j=-M}^{M} \sum_{q=-M}^{M} X_j X_q^* G_n^{jq}\right] \quad (5.41)$$

where R_n has been defined in Eq. (5.30), and F_n^j and G_n^{jq} are the n-th elements of the following two vectors, respectively.

$$\{F^j\} = -[K_1(k - j\nu)]^{-1}[K_2]\,[K_1(k)]^{-1}\{P\}\ e^{-i(k - j\nu)x} \quad (5.42)$$

$$\{G^{jq}\} = [K_1(k - j\nu + q\nu)]^{-1}[K_2]\,[K_1(k - j\nu)]^{-1}[K_2]\,[K_1(k)]^{-1}\{P\}\ e^{-i(k - j\nu + q\nu)x} \quad (5.43)$$

Now, if the random variables X_j, $j = 1,2,\cdots,M$, have zero means; i.e.,

$$E[X_j] = 0, \quad j = -M, \cdots, -1, 1, \cdots, M \quad (5.44)$$

then the mean value of the wave-number response function H is

$$E[H] = \sum_{n=1}^{N} \sin\frac{n\pi y}{b}\left\{R_n + \epsilon^2 \sum_{j=-M}^{M} \sum_{q=-M}^{M} E[X_j X_q^*] G_n^{jq}\right\} \quad (5.45)$$

We note that the first term on the right side of Eq. (5.45) is the same as the wave-number response function for the ideal

uniform tension membrane, (5.29), and the second term gives the contribution from the random variation in the tension field. The cross-spectrum of the response function H is

$$E[H(x_1,k,y_1,y_1',\omega)\ H^*(x_2,k,y_2,y_2',\omega)]$$

$$= \sum_{n=1}^{N}\sum_{\ell=1}^{N} \sin\frac{n\pi y_1}{b} \sin\frac{\ell\pi y_2}{b}\{R_n\ R_\ell^* + \epsilon^2 \sum_{j=-M}^{M}\sum_{q=-M}^{M} E[X_j\ X_q^*]\ [F_n^j\ F_\ell^{q*} + R_n\ G_\ell^{qj*} + G_n^{jq}\ R_\ell^*]\} \qquad (5.46)$$

where x_1 and y_1' should be substituted into the variables with the subscript n and x_2 and y_2' should be substituted into those with the subscript ℓ.

For the special case where X_j are statistically independent of each other and identically distributed random variables, and

$$E[X_j\ X_q^*] = \begin{cases} \sigma^2, & j = q \\ 0, & j \neq q \end{cases} \qquad (5.47)$$

Eqs. (5.45) and (5.46) reduce to, respectively,

$$E[H] = \sum_{n=1}^{N} \sin\frac{n\pi y}{b}\{R_n + \frac{V_T^2\ T_0^2}{2M} \sum_{j=-M}^{M} G_n^{jj}\} \qquad (5.48)$$

$$E[H\ H^*] = \sum_{n=1}^{N}\sum_{\ell=1}^{N} \sin\frac{n\pi y_1}{b} \sin\frac{\ell\pi y_2}{b}\{R_n\ R_\ell^* + \frac{V_T^2\ T_0^2}{2M} \sum_{j=-M}^{M} [F_n^j\ F_\ell^{j*} + R_n G_\ell^{jj*} + G_n^{jj}\ R_\ell^*]\} \qquad (5.49)$$

where
$$V_T = \frac{\epsilon\sqrt{2M}\sigma}{T_0} \tag{5.50}$$
is the coefficient of variation of the random tension in the y-direction. We note that due to the assumption of uncorrelated X_j, Eq. (5.49) becomes linear in each harmonic component of random tension field in the sense that the solution can be obtained by solving for each harmonic tension field variation separately and then superimposed to obtain the total correlation.

Now, the cross-spectrum of the structural response can be obtained by substituting into Eq. (2.52). Generally the integration over k in Eq. (2.52) must be performed numerically, but the integrations over y_1' and y_2' can often be calculated analytically. To illustrate we shall assume that the decay factor of the pressure field in the y-direction, $\psi_2(y_1' - y_2')$, can be expressed as
$$\psi_2(y_1' - y_2') = \exp(-|y_1' - y_2'|/Q) \tag{5.51}$$
where Q is an experimentally determined turbulence scale. Substitution of Eqs. (5.49) and (5.51) into Eq. (2.52) results in

$$\Phi_w(x_1, x_2, y_1, y_2, \omega)$$
$$= \bar{\Phi}_p(0,0,\omega) \int_{-\infty}^{\infty} \Psi_1(k - \frac{\omega}{U_c}) \{ \sum_{n=1}^{N} \sum_{\ell=1}^{N} \sin \frac{n\pi y_1}{b} \sin \frac{\ell\pi y_2}{b}$$
$$\sum_{s=1}^{N} \sum_{t=1}^{N} [U_{ns}(x_1)\, U_{\ell t}^{*}(x_2) + \frac{V_T^2 T_0^2}{2M} \sum_{j=-M}^{M}$$

$$(V_{ns,j}(x_1)\, V^*_{\ell t,j}(x_2) + U_{ns}(x_1)\, W^*_{\ell t,j}(x_2)$$

$$+ W_{ns,j}(x_1)\, U^*_{\ell t}(x_2)\,)]\}\, I_{st}\, dk \qquad (5.52)$$

where U_{ns}, $V_{ns,j}$, and $W_{ns,j}$ are the elements in the n-th row and s-th column of the following matrices, respectively.

$$[U(x)] = \left(\frac{2}{b}\right) [K_1(k)]^{-1}\, e^{-ikx} \qquad (5.53)$$

$$[V_j(x)] = -\left(\frac{2}{b}\right) [K_1(k - j\nu)]^{-1}[K_2]\,[K_1(k)]^{-1}$$

$$e^{-i(k - j\nu)x} \qquad (5.54)$$

$$[W_j(x)] = \left(\frac{2}{b}\right) [K_1(k)]^{-1}[K_2]\,[K_1(k - j\nu)]^{-1}[K_2]$$

$$[K_1(k)]^{-1}\, e^{-ikx} \qquad (5.55)$$

and

$$I_{st} = \frac{1}{(1/Q)^2 + (s\pi/b)^2}\,\frac{b}{Q}\,\delta_{st}$$

$$+ \frac{s\pi/b}{(1/Q)^2 + (s\pi/b)^2}\,\frac{t\pi/b}{(1/Q)^2 + (t\pi/b)^2}$$

$$\{1 - [(-1)^s + (-1)^t]\, e^{-b/Q} + (-1)^{s+t}\} \qquad (5.56)$$

In carrying out the numerical computations the most time-consuming part is the inversion of matrix K_1 beside the numerical integration over k which cannot be avoided. Therefore, in the actual computation, only the diagonal terms of K_1 matrix will be kept to save the computer time. Hence the coupling of modes due to the effect of transmitted

pressure, p_2, will be neglected.

5.3 Numerical Example

The following physical data are used in the numerical calculation:

properties of the membrane (Mylar membrane):

ρ (density) = 1.39×10^3 Kg/m^3

t (thickness) = 8.89×10^{-6} m

m (mass per unit area) = ρt

T_0 (tension) = 61.29 N/m

b (width) = 0.127 m

V_T (coefficient of variation of random tension) = 0.1

ν (fundamental wave number of random tension harmonics) = π m^{-1}

properties of surrounding fluid media:

$\rho_1 = \rho_2$ = density = 1.23 Kg/m^3

$a_1 = a_2$ = speed of sound = 340.36 m/sec

U_∞ (free stream velocity on the upper side of the membrance) = 30.48 m/sec

d (cavity depth) = 2.54×10^{-2} m

properties of turbulence:

$$\bar{\Phi}_p(0,0,\omega) = \text{spectral density} = \frac{1}{2}\frac{\delta^*}{U_\infty}\sum_{n=1}^{3} A_n e^{-\frac{\delta^*}{U_\infty} K_n|\omega|}$$

U_c (characteristic convection velocity of the turbulence) = $0.8\, U_\infty$

$\psi_1(\xi)$ = decay factor in the x-direction = $e^{-\frac{|\xi|}{U_c \Theta}}$

$$\Psi_1\left(k - \frac{\omega}{U_c}\right) = \frac{1}{\pi U_c \theta\left[(1/U_c\theta)^2 + (k - \omega/U_c)^2\right]}$$

$\psi_2(\eta)$ = decay factor in the y-direction = $e^{-\frac{|\eta|}{\alpha\delta^*}}$

$(Q = \alpha\delta^*)$

δ^* (boundary-layer displacement thickness)

$= 0.001168 \times Re^{-0.2}$

$Re = U_\infty x/\nu$

$x = 0.609$ m

$\nu = 1.464 \times 10^{-5}$ m^2/sec

and experimentary determined constants

$A_1 = 0.240$ $\quad K_1 = 0.470$

$A_2 = 1.08$ $\quad K_2 = 3.0$

$A_3 = 1.80$ $\quad K_3 = 14.0$

$\alpha = 2$

θ (eddy lifetime) $= -(1.24 \times 10^{-3})\ (U_\infty/a_1)$
$+ 1.15 \times 10^{-3}$ sec

Fig. 5.2 shows the spectral densities of structural response at $x_1 = x_2$ (the spectral densities of structural response is homogeneous in the x-direction, hence it is not a function of x_1 or x_2) and $y_1 = y_2 = b/2$ with or without the random variation in the membrane tension computed under the assumption of a frozen-pattern turbulence (i.e., $\psi_1(\xi) = 1$). Furthermore, only two harmonic terms of the random tension field, corresponding to $\nu = \pi\ m^{-1}$ $(j = 1)$ and $-\nu = -\pi\ m^{-1}$ $(j = -1)$, have been included in the computation. We recall that the cross-correlation of the structural response is linear in each harmonic component of the random tension field

when the random amplitudes of the tension, X_j, are statistically uncorrelated with each other. The spectral density of the structural response in the absence of random tension shows no peak within the frequency range shown in the figure, while several peaks appear if the random tension is taken into account. This change in appearance can be explained as follows. Since the exciting pressure is assumed to be a frozen-pattern turbulence, the wave number k of the turbulence is related to the frequency by $k = \omega/U_c$. Without random tension the wave number of the response, μ, of an infinite membrane unsupported in the x-direction must be equal to ω/U_c. Therefore, the coincidence resonance [32] would occur when one of the diagonal elements of the influence coefficient matrix K_1 could become zero. If the induced pressures, p_1 and p_2, are neglected, this would happen when

$$- m\omega^2 + T_0\left(\frac{n\pi}{b}\right)^2 + T_0\left(\frac{\omega}{U_c}\right)^2 = 0$$

However, numerical computations have shown that the left-hand side of this equation is always positive for any value of ω. Thus, coincidence can never occur when uniform tension T_0 is acting on the membrane alone. When the random tension terms are included in the computation, there appear perturbation terms which have factors of the form of $[K_1(k - j\nu)]^{-1}$, $j = \pm 1, \pm 2, \cdots$, in the wave-number response function H. Thus a shift of the wave number in the structural response from k to $k - j\nu$ occurs. When $j = 1$, the coincidence frequency

can be calculated from the equation

$$- m\omega^2 + T_0\left(\frac{n\pi}{b}\right)^2 + T_0\left(\frac{\omega}{U_c} - \nu\right)^2 = 0$$

For n = 1 and 2, this equation has solutions

$$f = 371 \text{ Hz}, 720 \text{ Hz}, \text{ for } n = 1$$
$$f = 425 \text{ Hz}, 665 \text{ Hz}, \text{ for } n = 2$$

No solution exists if n is greater than two. There is no coincidence resonance when j = -1. Note that these values are only rough estimates of the peak frequency since the induced pressure fields, p_1 and p_2, which have been ignored in the estimates provide additional inertia or stiffness to change the structural response, thus altering these peak frequencies.

Fig. 5.3 shows the spectral densities of structural response using the measured spectrum of turbulence pressure in the computation. Other specifications are the same as those used in obtaining Fig. 5.2. In this case, however, greater frequency intervals at every 50 Hz were used to save the computer time instead of 10 Hz interval in Fig. 5.2. Although the details are missing in this figure as compared to Fig. 5.2, the major effect of the random tension, which raises the spectrum values at some frequencies by several orders of magnitude, can be seen clearly. The comparison with Fig. 5.2 also shows that the frozen-pattern assumption

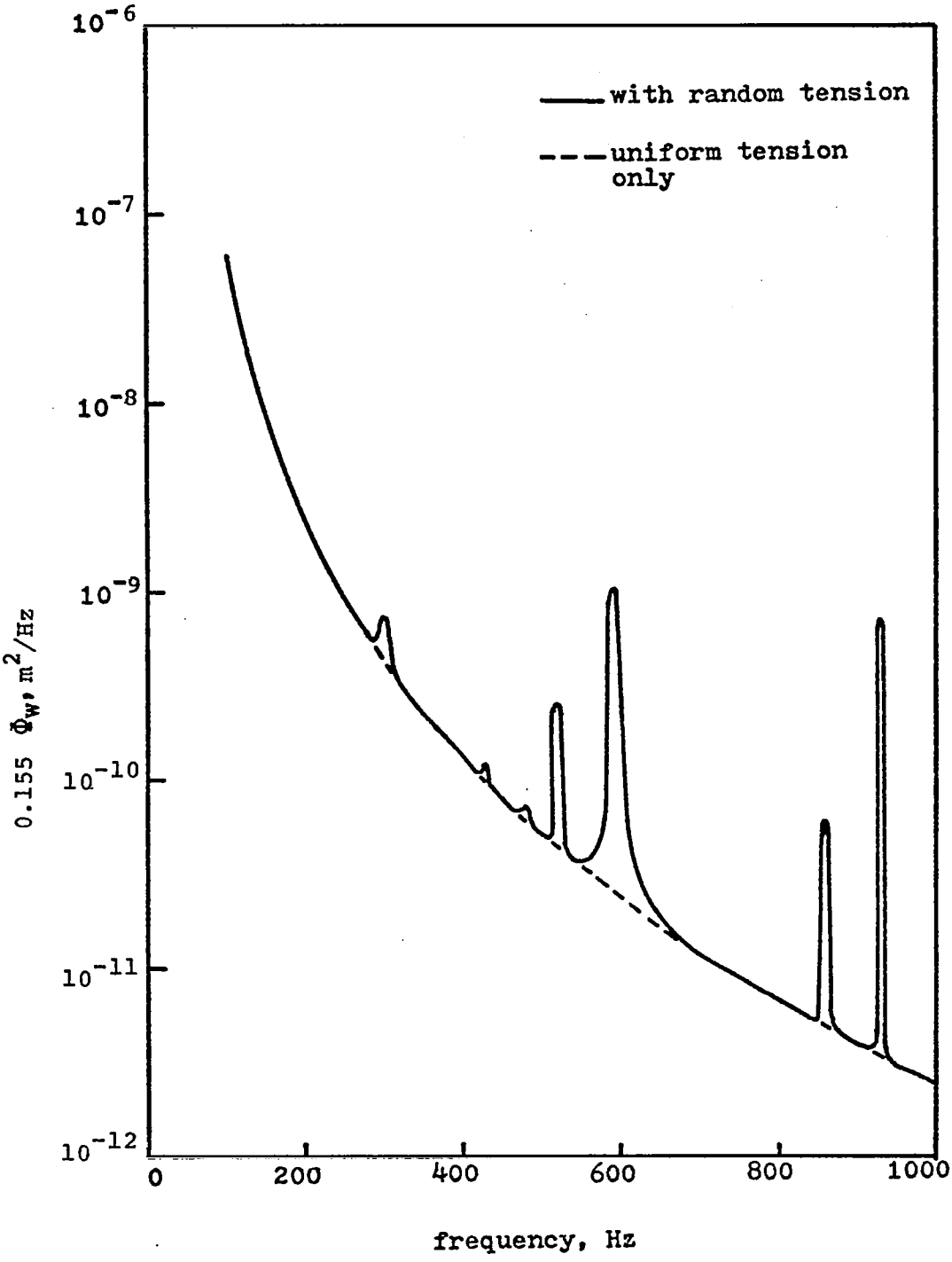

Fig. 5.2 Structural displacement spectrum under the frozen-pattern turbulence excitation

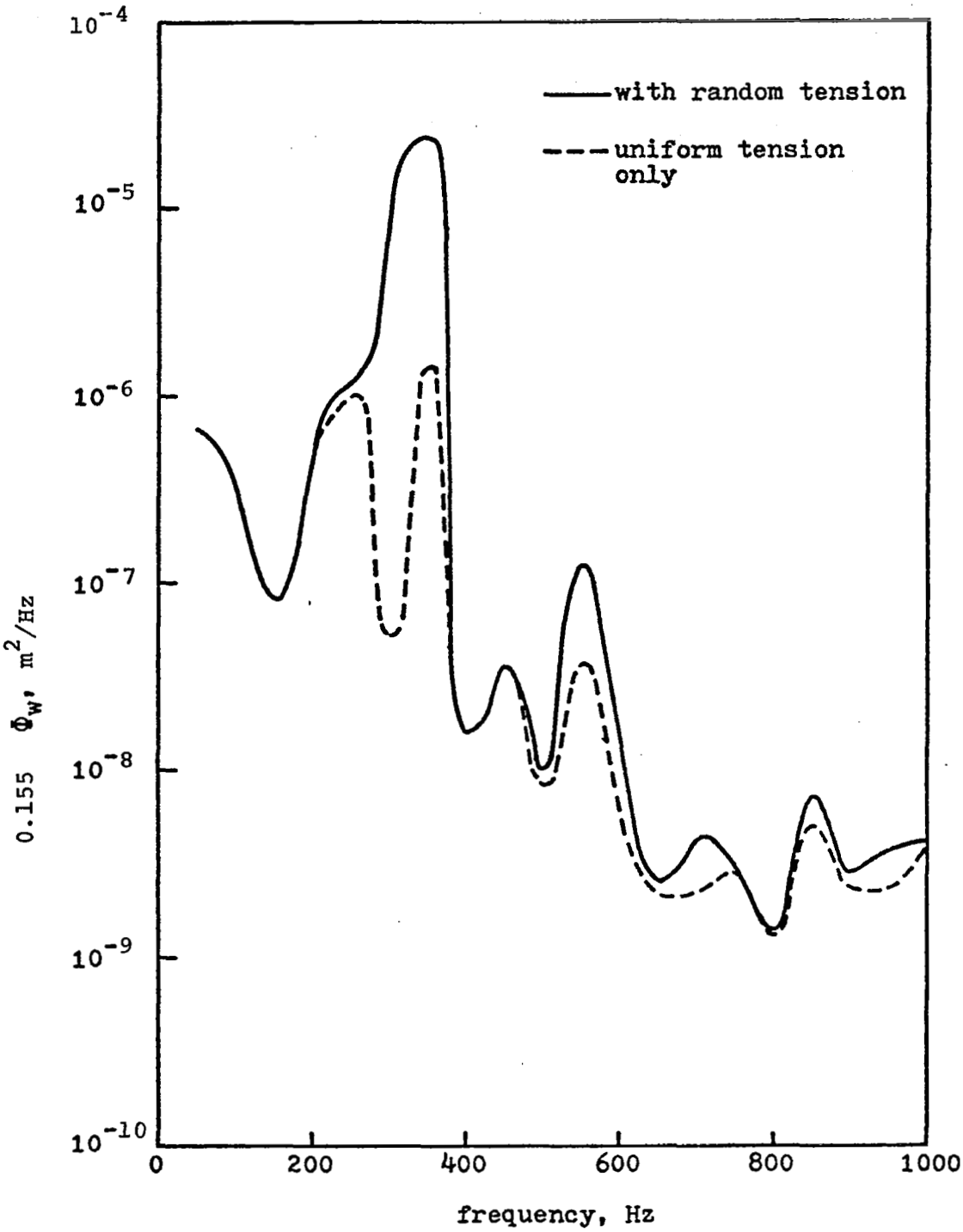

Fig. 5.3 Structural displacement spectrum under the decaying turbulence excitation

is unconservative, resulting in gross underestimates in the structural response calculation.

5.4 Conclusion

The turbulence decomposition scheme was applied to the two-dimensional problem of a membrane with random tension field. The Levy's series representation was used to describe the variation of the wave-number response function, H, in the y-direction. Therefore, integrations in the y-direction needed to calculate the cross-spectrum of the structural response could be carried out simply with only a single integration remaining to be done numerically on a computer. The effect of the randomness in the structural properties was also investigated, in particular the random non-uniform tension in the membrane. It has been shown that with a coefficient of variation of only 10% in the tension field the structural response spectrum may be increased by several orders of magnitude at some frequencies. The variation of the tension field need not be accidental, but it may be caused intentionally to create a spectral peak, for example, beneficial to skin-friction reduction. This proposition may be investigated in the future. The suitability of the frozen-pattern assumption was, again, examined in this chapter and the same conclusion as in Chapter III was drawn; namely, it leads to underestimation of structural response and omission of some important peaks in the spectral density of the response. Thus, the use of the frozen-pattern assumption should be avoided for

the analysis of the structural response spectra under the boundary-layer turbulence excitation.

In Chapter III-V, the emphasis has been placed on structural motions. In the next chapter our focus will be shifted to the skin-friction drag reduction itself.

VI. REYNOLDS STRESS ON A COMPLIANT SURFACE

6.1 Introduction

From observing the swimming of dolphins and amazed by the smooth motion of the fish Kramer hypothesized that favorable interactions between the flabby skin of the fish and water could reduce the skin-friction drag on the fish. Since then many researches, experimental [36-37] as well as theoretical [38-41], have been carried out in this field to find the mechanism of this highly applicable phenomenon. Aircraft and ship designers are especially interested in this problem since reduction of skin-friction will result in a decrease in fuel consumption. It has been estimated that the skin-friction drag of an aircraft can be as high as 50% of the total drag. Although some experimental studies performed on very flexible membranes have indicated friction-drag reduction in fully turbulent boundary layers, the theoretical follow-up has not been as successful. For historical reviews of previous works the reader is referred to [36,37].

One requirement for a successful theoretical analysis is a thorough understanding of the complicated structural motion under the excitation of the boundary-layer turbulence [37], to which Chapters III-V of this thesis were directed. Another requirement is the knowledge of the changing flow field resulting from the structural motion. In this chapter a perturbation approach similar to that used by Ffowcs Williams [48] and Blick [41] will be applied to compute the

perturbation Reynolds stress near the structure-fluid interface. The analysis will be related directly to the two structural models considered in previous chapters. The first model, a one-dimensional unsupported beam will be used again to present the basic concepts, and then these concepts will be applied to the more realistic model of a one-dimensional infinite beam on evenly spaced supports. In both cases the turbulence decomposition scheme will be utilized.

6.2 Theory

Fig. 6.1 shows a one-dimensional infinite beam which is basically the same beam considered in Chapter III. As the beam responds to excitations its motion will generate additional pressures in the fluid media on the upper and lower sides. As before, denoting these induced pressures by p_1 and p_2, respectively, the governing equation of the beam motion is given by

$$m \frac{\partial^2 w}{\partial t^2} + \eta \frac{\partial w}{\partial t} + EI \frac{\partial^4 w}{\partial x^4} - T \frac{\partial^2 w}{\partial x^2} = p + (p_1 - p_2)_{z=0} \quad (6.1)$$

Equation (6.1) differs from Eq. (3.1) in that a pre-tension T and a viscous damping coefficient η have been included.

The turbulence pressure field p can be expressed in the form previously introduced in Chapter II:

$$p(x,t) = \iint_{-\infty}^{\infty} e^{i(ukt - kx)} \, dF(k,u) \, dG(u) \quad (6.2)$$

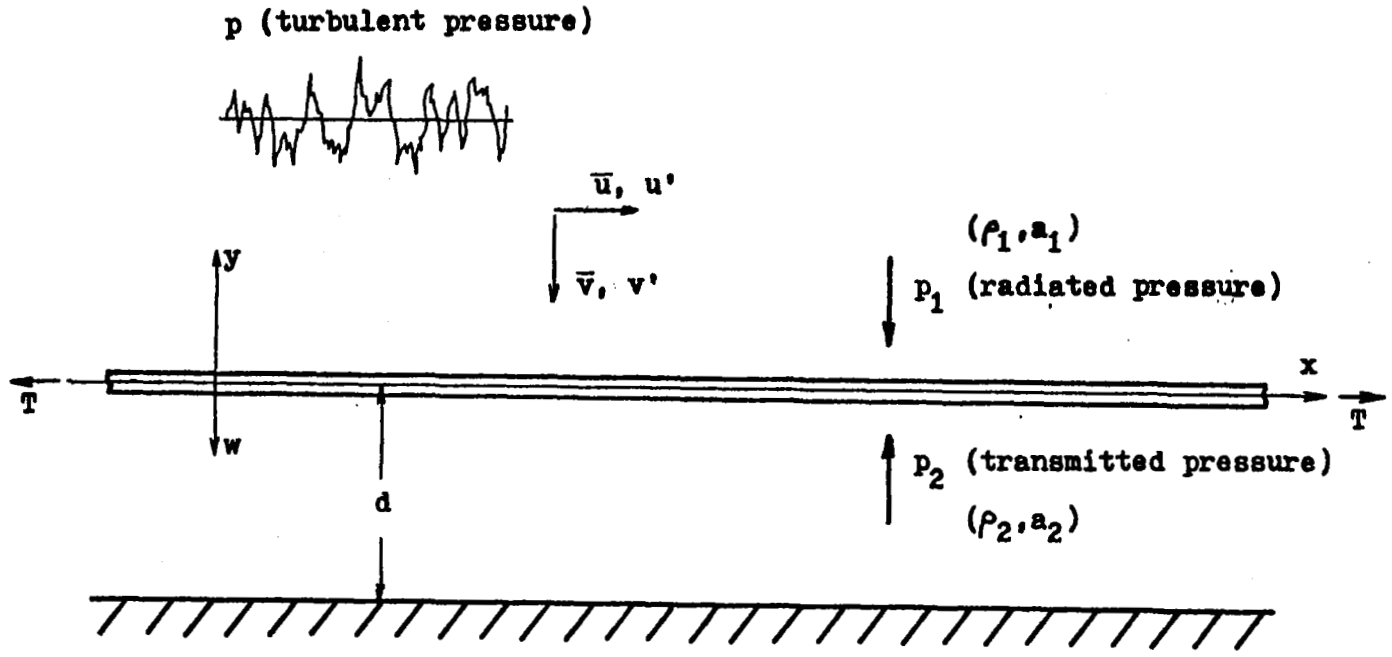

Fig. 6.1 One-dimensional infinite beam under the excitation of boundary-layer turbulence

The meaning of the functions F and G has been discussed in Chapter II. We recall that in the integrand the circular frequency ω is related to the wave-number k and the component convection velocity u by the relationship $\omega = ku$. Now, the induced quantities w, p_1 and p_2 can be expressed as follows:

$$w(x,t) = \iint_{-\infty}^{\infty} H(k,u)\, e^{i(ukt - kx)}\, dF(k,u)\, dG(u) \qquad (6.3)$$

$$p_1(x,y,t) = \iint_{-\infty}^{\infty} P_1(k,u,y)\, e^{i(ukt - kx)} dF(k,u)\, dG(u) \qquad (6.4)$$

$$p_2(x,y,t) = \iint_{-\infty}^{\infty} P_2(k,u,y)\, e^{i(ukt - kx)} dF(k,u)\, dG(u) \qquad (6.5)$$

where H, P_1, and P_2 may be called the wave-number response functions for the structural displacement, the radiated pressure, and the transmitted sound, respectively.

To determine the radiated pressure on the upper side of the beam, p_1, we use the usual assumption that the additional pressure can be obtained without regard to the presence of the turbulent pressure p. Then, p_1 can be obtained in the same way as in Chapter III;

$$P_1(k,u,0) = \rho_1 a_1 \frac{k(u - U_\infty)^2}{\sqrt{a_1^2 - (u - U_\infty)^2}} H(k,u) \qquad (6.6)$$

where U_∞ denotes the free-stream velocity of the flow on the upper side of the beam. For the case of incompressible fluid, we let $a_1 \to \infty$. Then Eq. (6.6) reduces to

$$P_1(k,u,0) = \rho_1 k(u - U_\infty)^2 \, H(k,u) \tag{6.7}$$

Following the same procedure as in Chapter III, the pressure generated on the lower side of the beam is found to be

$$P_2(k,u,0) = \rho_2\omega^2 \frac{\cot(\sqrt{u^2 - a_2^2}\, kd/a_2)}{\sqrt{u^2 - a_2^2}\, k/a_2} H(k,u) \tag{6.8}$$

where the bottom wall of the cavity is assumed to be acoustically hard. Taking the limit $a_2 \to \infty$, we have the incompressible flow solution

$$P_2(k,u,0) = -\rho_2\omega^2 \frac{\coth(kd)}{k} H(k,u) \tag{6.9}$$

For what follows we shall restrict our attention to the incompressible case.

Substituting Eqs. (6.2)-(6.5), (6.7), and (6.9) into Eq. (6.1), one obtains

$$H(k,u) = \left[-m\omega^2 + i\eta\omega + Dk^4 + Tk^2 - \rho_1 k(u - U_\infty)^2 - \rho_2\omega^2 \frac{\coth(kd)}{k}\right]^{-1} \tag{6.10}$$

This equation is similar to those derived in [41,48], however, in these references the effects of the radiated pressure p_1 was not taken into account.

Let the velocity components of the turbulent boundary-layer flow on the upper side of the compliant plate be $\overline{u} + u'$ and $\overline{v} + v'$, where $\overline{u}$ and $\overline{v}$ are the velocity components when

the boundary is rigid and u' and v' are perturbation velocities induced by the structural motion. Now assume that the perturbation velocities, u' and v', can be expressed as power series in y:

$$u'(x,y,t) = \sum_{n=0}^{\infty} a_n(x,t)\, y^n \tag{6.11}$$

$$v'(x,y,t) = \sum_{n=0}^{\infty} b_n(x,t)\, y^n \tag{6.12}$$

From the conservation of mass of an incompressible fluid, we have

$$\frac{\partial u'}{\partial x} + \frac{\partial v'}{\partial y} = 0 \tag{6.13}$$

In order that this condition is satisfied the coefficients in Eqs. (6.11) and (6.12) must be related as follows:

$$b_n(x,t) = -\frac{1}{n}\frac{\partial a_{n-1}(x,t)}{\partial x} \qquad \text{for } n = 1,2,\cdots \tag{6.14}$$

Therefore, substituting Eq. (6.14) into Eq. (6.12), we have

$$v'(x,y,t) = b_0(x,t) - \sum_{n=1}^{\infty} \frac{1}{n}\frac{\partial a_{n-1}(x,t)}{\partial x}\, y^n \tag{6.15}$$

The boundary conditions at the beam surface are

$$\bar{u}(w) + u'(x,w,t) = 0 \tag{6.16}$$

$$\bar{v}(w) + v'(x,w,t) = \frac{\partial w(x,t)}{\partial t} \tag{6.17}$$

Taking Taylor expansions of $\bar{u}(w)$ and $\bar{v}(w)$ about $y = 0$, and

neglecting the high order terms of w, one obtains

$$\bar{u}(w) = \bar{u}(0) + \left(\frac{\partial \bar{u}}{\partial y}\right)_{y=0} w + \cdots \approx \left(\frac{\partial \bar{u}}{\partial y}\right)_{y=0} w \qquad (6.18)$$

$$\bar{v}(w) = \bar{v}(0) + \left(\frac{\partial \bar{v}}{\partial y}\right)_{y=0} w + \cdots \approx 0 \qquad (6.19)$$

since $\bar{u}(0)$ and $\bar{v}(0)$ are zero and the continuity of the unperturbed fluid requires that

$$\left(\frac{\partial \bar{v}}{\partial y}\right)_{y=0} = -\left(\frac{\partial \bar{u}}{\partial x}\right)_{y=0} = 0$$

Substituting Eqs. (6.11) and (6.18) into Eq. (6.16), one obtains

$$a_0(x,t) + a_1(x,t)w + a_2(x,t)w^2 + \cdots = -\left(\frac{\partial \bar{u}}{\partial y}\right)_{y=0} w \qquad (6.20)$$

Keeping only the first term on the left-hand side of this equation, we have

$$a_0(x,t) = -Uw \qquad (6.21)$$

where U is defined as

$$U = \left(\frac{\partial \bar{u}}{\partial y}\right)_{y=0} \qquad (6.22)$$

In a similar way we obtain from Eqs. (6.15), (6.17) and (6.19),

$$b_0(x,t) - \frac{\partial a_0(x,t)}{\partial x} w - \frac{1}{2} \frac{\partial a_1(x,t)}{\partial x} w^2 - \cdots = \frac{\partial w}{\partial t} \qquad (6.23)$$

Again, retaining only the first term on the left-hand side,

$$b_0(x,t) = \frac{\partial w}{\partial t} \tag{6.24}$$

Equation (6.24) confirms what might have been concluded from intuitive reasoning that the perturbed velocity in the y-direction is equal to the structural motion in that direction. Substituting Eqs. (6.21) and (6.24) into Eqs (6.11) and (6.15), we have

$$u'(x,y,t) = - Uw(x,t) + \sum_{n=1}^{\infty} a_n(x,t)y^n \tag{6.25}$$

$$v'(x,y,t) = \frac{\partial w(x,t)}{\partial t} + U \frac{\partial w(x,t)}{\partial x} y - \sum_{n=2}^{\infty} \frac{1}{n} \frac{\partial a_{n-1}(x,t)}{\partial x} y^n \tag{6.26}$$

In addition to the continuity equation and the boundary conditions, the velocity components in the flow field must satisfy two momentum equations, one in the x-direction and the other in the y-direction. However, it is sometimes more convenient to replace one of these two equations by a diffusion equation governing the vorticity perturbation.

$$\omega'(x,y,t) = \frac{\partial v'}{\partial x} - \frac{\partial u'}{\partial y} \tag{6.27}$$

In the proximity of the structure this diffusion equation is given by

$$\frac{\partial \omega'}{\partial t} = \nu\left(\frac{\partial^2}{\partial x^2} + \frac{\partial^2}{\partial y^2}\right) \omega' \tag{6.28}$$

where ν represents the coefficient of viscosity. We shall apply this diffusion equation next to calculate the higher order coefficients in the power series of u' and v'. Since ω' results from the structural motion it can be expressed in a form similar to Eqs. (6.2)-(6.5); i.e.,

$$\omega'(x,y,t) = \iint_{-\infty}^{\infty} \Omega(k,u,y)\, e^{i(ukt - kx)}\, dF(k,u)\, dG(u) \tag{6.29}$$

Substituting this expression into Eq. (6.28), we have

$$\frac{\partial^2}{\partial y^2}\Omega(k,u,y) - (k^2 + \frac{iuk}{\nu})\,\Omega(k,u,y) = 0 \tag{6.30}$$

with the condition that the vorticity vanishes at infinity. A solution for this differential equation may be expressed as

$$\Omega(k,u,y) = \overline{\Omega}(k,u)\, \exp[-(k^2 + \frac{iuk}{\nu})^{\frac{1}{2}}\, y] \tag{6.31}$$

where the function $\overline{\Omega}$ is to be determined. Expanding the exponential function on the right-hand side of Eq. (6.31) in a Taylor series about y=0, one obtains

$$\exp[-(k^2 + \frac{iuk}{\nu})^{\frac{1}{2}} y] = \sum_{n=0}^{\infty} \frac{y^n}{n!}\,(-1)^n\,(k^2 + \frac{iuk}{\nu})^{\frac{n}{2}}$$

Therefore, Eq. (6.29) can be written as

$$\omega'(x,y,t) = \iint_{-\infty}^{\infty} \overline{\Omega}(k,u) \sum_{n=0}^{\infty} \frac{y^n}{n!}\,(-1)^n\,(k^2 + \frac{iuk}{\nu})^{\frac{n}{2}}$$
$$e^{i(ukt - kx)}\, dF(k,u)\, dG(u) \tag{6.32}$$

However, from Eqs. (6.25)-(6.27)

$$\omega'(x,y,t) = \frac{\partial^2 w(x,t)}{\partial t\, \partial x} - a_1(x,t) + [\frac{\partial^2 w(x,t)}{\partial x^2} U - 2a_2(x,t)]y + \cdots \tag{6.33}$$

In consistence with the representations of w and ω', Eqs. (6.3) and (6.29), each a_n also can be expressed as follows:

$$a_n(x,t) = \iint_{-\infty}^{\infty} A_n(k,u)\, e^{i(ukt - kx)}\, dF(k,u)\, dG(u) \tag{6.34}$$

Substituting this equation and Eq. (6.3) into Eq. (6.33),

$$\omega'(x,y,t) = \iint_{-\infty}^{\infty} [uk^2 H(k,u) - A_1(k,u) - Uk^2 H(k,u)y - 2A_2(k,u)y]\, e^{i(ukt - kx)}\, dF(k,u)\, dG(u) + \text{higher order terms in } y \tag{6.35}$$

By equating coefficients of y^n in Eqs. (6.32) and (6.35), we obtain

$$\overline{\Omega}(k,u) = uk^2 H(k,u) - A_1(k,u) \tag{6.36}$$

$$\overline{\Omega}(k,u)\, (k^2 + \frac{iuk}{\nu})^{\frac{1}{2}} = Uk^2 H(k,u) + 2A_2(k,u) \tag{6.37}$$

Eliminating $\overline{\Omega}$ from these two equations, we have

$$A_1(k,u) = uk^2 H(k,u) - (k^2 + \frac{iuk}{\nu})^{-\frac{1}{2}} [Uk^2 H(k,u)$$

$$+ 2A_2(k,u)] \tag{6.38}$$

To calculate A_1 and A_2 we use the momentum equation in the x-direction

$$\frac{\partial(\bar{u} + u')}{\partial t} + (\bar{u} + u') \frac{\partial(\bar{u} + u')}{\partial x} + (\bar{v} + v') \frac{\partial(\bar{u} + u')}{\partial y}$$

$$= -\frac{1}{\rho_1} \frac{\partial(p + p_1)}{\partial x} + \nu\nabla^2(\bar{u} + u') \tag{6.39}$$

However, for the rigid wall case, we have

$$\frac{\partial\bar{u}}{\partial t} + \bar{u} \frac{\partial\bar{u}}{\partial x} + \bar{v} \frac{\partial\bar{u}}{\partial y} = -\frac{1}{\rho_1} \frac{\partial p}{\partial x} + \nu\nabla^2\bar{u} \tag{6.40}$$

Thus, by subtracting Eq. (6.40) from Eq. (6.39) and neglecting the square terms of perturbation velocities, one obtains

$$\frac{\partial u'}{\partial t} + \bar{u} \frac{\partial u'}{\partial x} + u' \frac{\partial\bar{u}}{\partial x} + \bar{v} \frac{\partial u'}{\partial y} + v' \frac{\partial\bar{u}}{\partial y} = -\frac{1}{\rho_1} \frac{\partial p_1}{\partial x} + \nu\nabla^2 u' \tag{6.41}$$

It has been shown in Eqs. (6.18) and (6.19) that at the proximity of the beam $\bar{u}$ and $\bar{v}$ can be approximated as follows:

$$\bar{u}(y) = \bar{u}(0) + \left(\frac{\partial\bar{u}}{\partial y}\right)_{y=0} y + \cdots = Uy$$

$$\bar{v}(y) = \bar{v}(0) + \left(\frac{\partial\bar{v}}{\partial y}\right)_{y=0} y + \cdots = 0$$

Thus, the Navier-Stokes equation for the perturbation velocities near the compliant surface can be approximated as

$$\frac{\partial u'}{\partial t} + Uy \frac{\partial u'}{\partial x} + v'U = -\frac{1}{\rho_1} \frac{\partial p_1}{\partial x} + \nu \nabla^2 u' \qquad (6.42)$$

Substituting Eqs. (6.4), (6.25), (6.26), and (6.34) in Eq. (6.42) and letting y = 0, we obtain

$$\frac{1}{\rho_1} ikP_1(k,u,0) = -\nu[Uk^2 H(k,u) + 2A_2(k,u)] \qquad (6.43)$$

Therefore

$$A_2(k,u) = -\frac{ik}{2\nu\rho_1} P_1(k,u,0) - \frac{U}{2} k^2 H(k,u) \qquad (6.44)$$

Eliminating $A_2(k,u)$ from Eqs. (6.38) and (6.44),

$$A_1(k,u) = uk^2 H(k,u) + \frac{ik}{\nu\rho_1} (k^2 + \frac{iuk}{\nu})^{-\frac{1}{2}} P_1(k,u,0) \qquad (6.45)$$

Now, substituting Eqs. (6.3), (6.44), and (6.45) into Eqs. (6.25) and (6.26), we have

$$u'(x,y,t) = \iint_{-\infty}^{\infty} B(k,u,y)\, e^{i(ukt - kx)}\, dF(k,u)\, dG(u) \qquad (6.46)$$

$$v'(x,y,t) = \iint_{-\infty}^{\infty} C(k,u,y)\, e^{i(ukt - kx)}\, dF(k,u)\, dG(u) \qquad (6.47)$$

where

$$B(k,u,y) = -UH(k,u) + \{uk^2 H(k,u) + \frac{ik}{\nu\rho_1} (k^2 + \frac{iuk}{\nu})^{-\frac{1}{2}} P_1(k,u,0)\}y + \text{higher order terms in } y \qquad (6.48)$$

$$C(k,u,y) = iukH(k,u) - ikUH(k,u)y$$

$$+ \text{higher order terms in } y \qquad (6.49)$$

The Reynolds stress associated with the perturbation velocities, u' and v', is defined as[#]

$$\tau(x,y) = \rho_1 E\{u'v'\} \qquad (6.50)$$

The usual minus sign associated with the definition of the Reynolds stress is dropped here since, as shown in Fig. 6.1, the positive v' is taken to be opposite to the conventional direction. Now, substituting Eqs. (6.46) through (6.49) into Eq. (6.50) and applying Eq. (2.26), one obtains

$$\tau(y) = \iint_{-\infty}^{\infty} T(k,u,y)\, S_p(k,u)\, dk\, du \qquad (6.51)$$

in which

$$T(k,u,y) = \rho_1 iukUHH^* + \rho_1[-ikU^2HH^* - iu^2k^3HH^*$$

$$+ \frac{uk^2}{\nu\rho_1}\left(k^2 + \frac{iuk}{\nu}\right)^{-\frac{1}{2}} P_1 H^*]y$$

$$+ \text{higher order terms in } y \qquad (6.52)$$

Since $\omega = ku$ and the wave-number spectrum of the turbulence

---

In theory, the imaginary parts in the expressions for u' and v' should be zero; however, some approximations have been used in the analysis which may lead to non-zero imaginary parts in these expressions. Such superfluous terms should be discarded in calculating the Reynolds stress. Therefore, instead of Eq. (6.50) one can write

$$\tau(x,y) = \rho_1 E[\mathrm{Re}(u')\ \mathrm{Re}(v')]$$

pressure, S_p, can be expressed in terms of the frequency spectrum using Eq. (2.33), Eq. (6.51) can be changed also to

$$\tau(y) = \iint_{-\infty}^{\infty} T(k,\frac{\omega}{k},y)\ \bar{\Phi}_p(0,\omega)\ \Psi(k - \frac{\omega}{U_c})\ dk\ d\omega \qquad (6.53)$$

where $\bar{\Phi}_p(0,\omega)$ denotes the frequency spectrum of the turbulence pressure and Ψ accounts for the decay property with respect to spatial separation. Due to statistical stationality and homogeneity of the structural motion, the first three terms in the right-hand side of Eq. (6.53) vanish. Thus the expression for the Reynolds stress reduces to

$$\tau(y) = \iint_{-\infty}^{\infty} \frac{\omega k}{\nu}\ (k^2 + \frac{i\omega}{\nu})^{-\frac{1}{2}} P_1(k,\frac{\omega}{k},0)\ H^*(k,\frac{\omega}{k})\ y$$
$$\bar{\Phi}_p(0,\omega)\ \Psi(k - \frac{\omega}{U_c})\ dk\ d\omega \qquad (6.54)$$

We now define a Reynolds number, R, based on the wave convection velocity ω/k and the wavelength $2\pi/k$;

$$R = \frac{(\omega/k)(2\pi/k)}{2\pi\nu} = \frac{\omega}{\nu k^2} \qquad (6.55)$$

Assuming this Reynolds number, R, is large, the square-root in the integrand of Eq. (6.54) is expanded in a Taylor series about $1/R = 0$;

$$(k^2 + \frac{i\omega}{\nu})^{-\frac{1}{2}} = \sqrt{\frac{\nu}{i\omega}}\ (1 + \frac{1}{iR})^{-\frac{1}{2}}$$
$$= \sqrt{\frac{\nu}{i\omega}}\ (1 + \frac{i}{2R} + \cdots) \qquad (6.56)$$

For values of R much greater than unity, the first term of the series alone is adequate, Thus,

$$\tau(y) = \iint_{-\infty}^{\infty} \frac{\omega k}{\sqrt{i\nu\omega}} P_1(k,\tfrac{\omega}{k},0)\ H^*(k,\tfrac{\omega}{k})\ y$$

$$\overline{\Phi}_p(0,\omega)\ \Psi(k - \tfrac{\omega}{U_c})\ dk\ d\omega \qquad (6.57)$$

This expression of the Reynolds stress differs from Eq. (33) in [48] in that the radiation pressure, P_1, takes place of the pressure fluctuation. As shown in the process of obtaining Eq. (6.42), the radiation pressure is more directly related to the perturbation velocities and, therefore, to the perturbation Reynolds stress than the unperturbed turbulence pressure on the rigid wall. Thus, this expression of the Reynolds stress seems to be more plausible than that in [41,48].

Now, substitutiong Eqs. (6.7) and (6.10) into Eq. (6.57), and keeping only the real part which represents the physical Reynolds stress, we have

$$\tau(y) = \iint_{-\infty}^{\infty} \frac{\rho_1 \omega k^2}{\sqrt{2\nu|\omega|}} (\tfrac{\omega}{k} - U_\infty)^2 \{[-m\omega^2 + Dk^4 + Tk^2$$

$$- \rho_1 k(\tfrac{\omega}{k} - U_\infty)^2 - \rho_2 \omega^2 \frac{\coth(kd)}{k}]^2 + \eta^2\omega^2\}\ y$$

$$\overline{\Phi}_p(0,\omega)\ \Psi(k - \tfrac{\omega}{U_c})\ dk\ d\omega \qquad (6.58)$$

It is clear from Eq. (6.54) that the perturbation Reynolds stress vanishes when there is no pressure radiation; i.e., $P_1(k,\frac{\omega}{k},0) = 0$. This happens when the wave propagation speed of the structural motion, ω/k, becomes equal to the free-stream velocity of the flow, U_∞. Of course, in the absence of structural motion the perturbation Reynolds stress also must be zero.

If the beam motion is favorable the Reynolds stress may become negative. It has been suggested [48] that such a negative Reynolds stress in the vicinity of the surface may deprive the turbulence in the boundary layer with energy supply and, therefore, the turbulence level may decrease. As seen in Eq. (6.58) the sign of the perturbation Reynolds stress can be altered by changing the structural properties. However, the relationship is subtle and extensive numerical studies would be required to reach any quantitative conclusions.

6.3 Periodically Supported Beam

The structural model used in the preceding section for a preliminary investigation of the change in the Reynolds stress in the fluid due to structural motion was an unsupported infinite beam. However the results obtained there can be extended easily to the case of periodically supported infinite beam. This model is shown in Fig. 6.2, and it resembles more realistically the construction of an airplane fuselage.

The governing equation of the beam motion not directly on the support is given by

$$m\frac{\partial^2 w}{\partial t^2} + \eta\frac{\partial w}{\partial t} + D(1 + ig)\frac{\partial^4 w}{\partial x^4} - T\frac{\partial^2 w}{\partial x^2}$$

$$= p + (p_1 - p_2)_{y=0} \qquad (6.59)$$

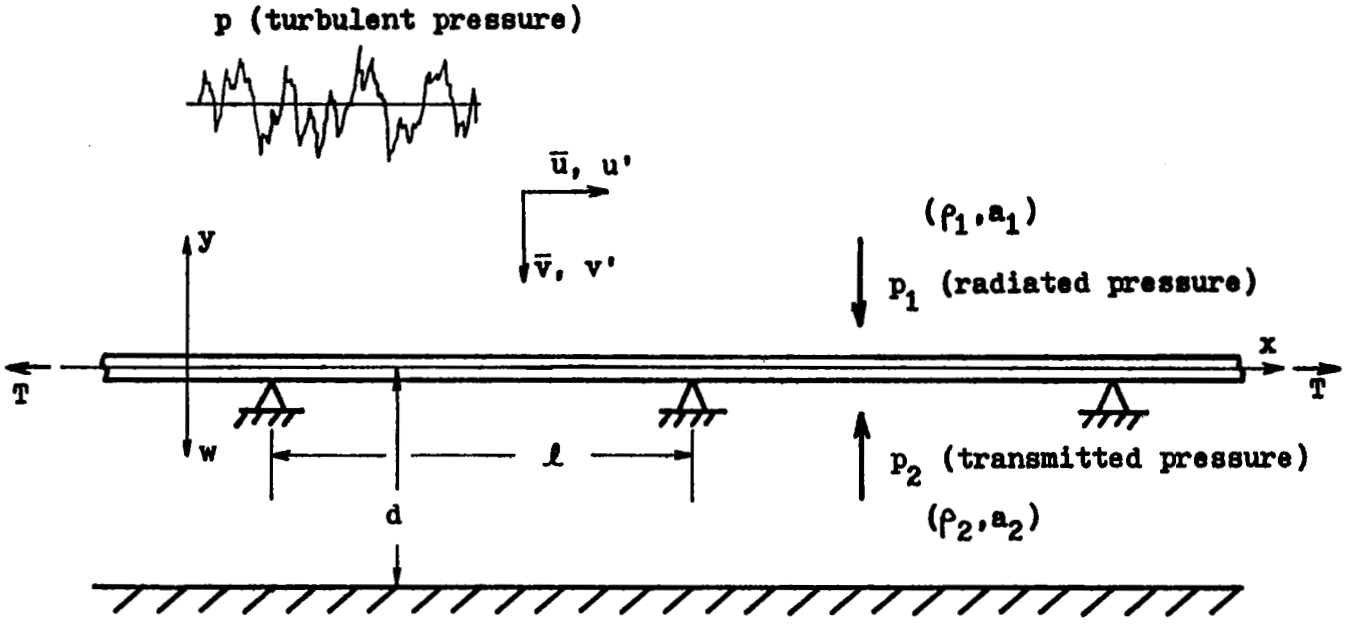

Fig. 6.2 One-dimensional periodic beam under the excitation of boundary-layer turbulence

where η denotes the viscous damping coefficient, g is the loss factor of the beam material, D is the beam rigidity, and m, T, p_1 and p_2 are the same symbols used in the preceding section. For the purpose of determining the wave-number response function, H(x,k,u), the turbulent pressure p should be replaced by exp[i(ukt - kx)] and the structural response w equated with H(x,k,u) exp(iukt). Other induced quantities should also be replaced by their wave-number response functions in the same manner.

Since the supports give rise to multiple reflections of the propagation wave in the structure, the same expression for the wave-number response function H as that used in Chapter IV is suitable; i.e.,

$$H(x,k,u) = \sum_{n=-\infty}^{\infty} H_n \exp(-i\mu_n x/\ell) \tag{6.60}$$

where

$$\mu_n = \mu_0 + 2n\pi = k\ell + 2n\pi \tag{6.61}$$

The radiated pressure p_1 is governed by the equation

$$\left(\frac{\partial}{\partial t} + U_\infty \frac{\partial}{\partial x}\right)^2 p_1 - a_1^2 \left(\frac{\partial^2}{\partial x^2} + \frac{\partial^2}{\partial y^2}\right) p_1 = 0 \tag{6.62}$$

and subject to the conditions that p_1 can propagate only in the region $y > 0$, and that

$$\left(\frac{\partial p_1}{\partial y}\right)_{y=0} = \rho_1 \left(iku + U_\infty \frac{\partial}{\partial x}\right)^2 H\, e^{iukt} \tag{6.63}$$

The solution of this system, when evaluated at y=0, is given by

$$p_1 = -i\rho_1 a_1 \sum_{n=-\infty}^{\infty} H_n \frac{(u_n - U_\infty)^2}{(\frac{\ell}{\mu_n})[(u_n - U_\infty)^2 - a_1^2]^{\frac{1}{2}}}$$

$$e^{i(ukt - \mu_n x/\ell)} \tag{6.64}$$

where

$$u_n = uk\ell/\mu_n \tag{6.65}$$

The solution for the case of incompressible flow can be obtained by taking the limit $a_1 \to \infty$; i.e.

$$p_1 = \sum_{n=-\infty}^{\infty} P_{1n} e^{i(ukt - \mu_n x/\ell)} \tag{6.66}$$

where

$$P_{1n} = \rho_1 (\frac{\mu_n}{\ell}) (\frac{uk\ell}{\mu_n} - U_\infty)^2 H_n \tag{6.67}$$

The transmitted pressure p_2 in the fluid medium $-d \leq y < 0$ is governed by

$$\frac{\partial^2 p_2}{\partial t^2} - a_2^2 (\frac{\partial^2}{\partial x^2} + \frac{\partial^2}{\partial y^2}) p_2 = 0 \tag{6.68}$$

and subject to the conditions

$$\frac{\partial p_2}{\partial y} = 0 \qquad \text{at } y = -d \tag{6.69}$$

$$\frac{\partial p_2}{\partial y} = -\rho_2 (uk)^2 H e^{iukt} \qquad \text{at } y = 0 \tag{6.70}$$

The solution for p_2, when evaluated at $y = 0$, is given by

$$p_2 = \rho_2(uk)^2 \sum_{n=-\infty}^{\infty} H_n \frac{\cot(\gamma_n d)}{\gamma_n} e^{i(ukt - \mu_n x/\ell)} \qquad (6.71)$$

where

$$\gamma_n^2 = (\frac{uk}{a_2})^2 - (\frac{\mu_n}{\ell})^2 \qquad (6.72)$$

Taking the limit $a_2 \to \infty$, Eq. (6.71) reduces to the incompressible flow solution

$$p_2 = -\rho_2(uk)^2 \sum_{n=-\infty}^{\infty} H_n \frac{\coth(\mu_n d/\ell)}{\mu_n/\ell} e^{i(ukt - \mu_n x/\ell)} \qquad (6.73)$$

At this point it is of interest to note that the H_n are not all independent of each other due to the constraints at the periodic simple supports. At these supports the deflections are zero. Thus by substituting $x = 0$ into Eq. (6.60),

$$H(0,k,u) = \sum_{n=-\infty}^{\infty} H_n = 0$$

or

$$H_0 = -\sum_{\substack{n=-\infty \\ n\neq 0}}^{\infty} H_n \qquad (6.74)$$

Hence, an alternative representation for H is

$$H(x,k,u) = \sum_{\substack{n=-\infty \\ n\neq 0}}^{\infty} H_n \left(e^{-i\mu_n x/\ell} - e^{-i\mu_0 x/\ell}\right) \qquad (6.75)$$

which is also a better representation from a computational point of view. Substituting Eqs. (6.66), (6.73) and (6.75) into Eq. (6.59), one obtains

$$\sum_{\substack{n=-\infty \\ n\neq 0}}^{\infty} [\varphi(n)\, e^{-i\mu_n x/\ell} - \varphi(0)\, e^{-i\mu_0 x/\ell}]\, H_n\, e^{iukt}$$

$$= e^{i(ukt - \mu_0 x/\ell)} \tag{6.76}$$

where

$$\varphi(n) = -m(uk)^2 + i\eta(uk) + D(1 + ig)\left(\frac{\mu_n}{\ell}\right)^4 + T\left(\frac{\mu_n}{\ell}\right)^2$$

$$- \rho_1 \left(\frac{\mu_n}{\ell}\right)\left(\frac{uk\ell}{\mu_n} - U_\infty\right)^2 - \rho_2 (uk)^2 \frac{\coth(\mu_n d/\ell)}{\mu_n/\ell} \tag{6.77}$$

To determine the coefficients H_n we apply the well-known virtual work principle. Specifically, we assume a virtual displacement

$$\delta w = \delta H_j\, [e^{i\mu_j x/\ell} - e^{i\mu_0 x/\ell}]\, e^{-iukt} \tag{6.78}$$

The virtual work done by the internal and external forces must sum up to zero. Due to the spatial periodicity of the structural response and the virtual displacement, it is only necessary to apply the virtual work principle to one periodic unit. Thus, multiplying δw to both sides of Eq. (6.76) and integrating over $0 < x < \ell$, we have

$$\varphi(j)\, H_j + \varphi(0) \sum_{\substack{n=-\infty \\ n\neq 0}}^{\infty} H_n = -1 \quad \text{for } j \neq 0 \tag{6.79}$$

Equation (6.79) shows that the product $\varphi(j)\, H_j$ is independent of j; i.e.,

$$\varphi(1)H_1 = \varphi(2)H_2 = \cdots = \varphi(j)H_j = \cdots$$

Thus, substituting

$$H_n = H_j\varphi(j)/\varphi(n) \tag{6.80}$$

into Eq. (6.79), we obtain an equation involving only one unknown

$$H_j\varphi(j)\varphi(0)\sum_{n=-\infty}^{\infty}\frac{1}{\varphi(n)} = -1 \quad \text{for } j \neq 0 \tag{6.81}$$

which is solved readily to give

$$H_j = -\left[\varphi(j)\varphi(0)\sum_{n=-\infty}^{\infty}\frac{1}{\varphi(n)}\right]^{-1} \quad \text{for } j \neq 0 \tag{6.82}$$

Denote the velocity components of the turbulent boundary-layer flow on the upper side of the beam again by $\bar{u} + u'$ and $\bar{v} + v'$ where $\bar{u}$ and $\bar{v}$ are the components corresponding to a rigid wall. In view of Eq. (6.60), the perturbation velocities, u' and v', can be expressed as power series in y as follows:

$$u'(x,y,t) = \sum_{n=0}^{\infty}\sum_{j=-\infty}^{\infty} A_{nj}y^n\, e^{i(ukt - \mu_j x/\ell)} \tag{6.83}$$

$$v'(x,y,t) = \sum_{n=0}^{\infty}\sum_{j=-\infty}^{\infty} B_{nj}y^n\, e^{i(ukt - \mu_j x/\ell)} \tag{6.84}$$

From Eqs. (6.83) and (6.84) and the continuity equation for

an incompressible fluid;

$$\frac{\partial u'}{\partial x} + \frac{\partial v'}{\partial y} = 0 \tag{6.85}$$

one obtains

$$\sum_{n=0}^{\infty} \sum_{j=-\infty}^{\infty} (i \frac{\mu_j}{\ell}) y^n A_{nj} e^{i(ukt - \mu_j x/\ell)}$$

$$= \sum_{n=1}^{\infty} \sum_{j=-\infty}^{\infty} n y^{n-1} B_{nj} e^{i(ukt - \mu_j x/\ell)} \quad n y^{n-1}$$

Multiplying both sides of the equation by $\exp(i\mu_j x/\ell)$ and integrating over $0 < x < \ell$, we have

$$B_{nj} = \frac{1}{n} (\frac{i\mu_j}{\ell}) A_{n-1,j} , \quad \text{for } n = 1,2, \cdots \tag{6.86}$$

Therefore, by substituting Eq. (6.86) into Eq. (6.84),

$$v'(x,y,t) = \sum_{j=-\infty}^{\infty} [B_{0j} + \sum_{n=1}^{\infty} \frac{1}{n} (\frac{i\mu_j}{\ell}) A_{n-1,j} y^n]$$

$$e^{i(ukt - \mu_j x/\ell)} \tag{6.87}$$

The non-slip condition on the plate surface can be stated as

$$\bar{u}(w) + u'(x,w,t) = 0 \tag{6.88}$$

and

$$\bar{v}(w) + v'(x,w,t) = \frac{\partial w(x,t)}{\partial t} \tag{6.89}$$

Taking Taylor expansions of $\bar{u}(w)$ and $\bar{v}(w)$ about $y = 0$, and neglecting the high order terms of w, we have

$$\bar{u}(w) = \left(\frac{\partial \bar{u}}{\partial y}\right)_{y=0} w \tag{6.90}$$

$$\bar{v}(w) = 0 \tag{6.91}$$

Substituting Eqs. (6.83) and (6.90) into Eq. (6.88), one obtains

$$\sum_{j=-\infty}^{\infty} (A_{0j} + A_{1j}w + A_{2j}w^2 + \cdots) e^{i(ukt - \mu_j x/\ell)}$$

$$= -\left(\frac{\partial \bar{u}}{\partial y}\right)_{y=0} \sum_{j=-\infty}^{\infty} H_j e^{i(ukt - \mu_j x/\ell)}$$

Keeping only the first term on the left-hand side of this equation, we have

$$A_{0j} = -U H_j \tag{6.92}$$

where

$$U = \left(\frac{\partial \bar{u}}{\partial y}\right)_{y=0} \tag{6.93}$$

Similarly, from Eqs. (6.87), (6.89) and (6.91),

$$B_{0j} = iukH_j \tag{6.94}$$

Now, substituting Eqs. (6.92) and (6.94) into Eqs. (6.83) and (6.87), we obtain

$$u'(x,y,t) = \sum_{j=-\infty}^{\infty}(-UH_j + \sum_{n=1}^{\infty} A_{nj}y^n)\, e^{i(ukt - \mu_j x/\ell)} \tag{6.95}$$

$$v'(x,y,t) = \sum_{j=-\infty}^{\infty}(iukH_j - \frac{i\mu_j}{\ell} UH_j y + \sum_{n=2}^{\infty} \frac{1}{n} \frac{i\mu_j}{\ell} A_{n-1,j}y^n)$$
$$e^{i(ukt - \mu_j x/\ell)} \tag{6.96}$$

The vorticity perturbation

$$\omega'(x,y,t) = \frac{\partial v'}{\partial x} - \frac{\partial u'}{\partial y} \tag{6.97}$$

must satisfy the diffusion equation near the beam;

$$\frac{\partial \omega'}{\partial t} = \nu(\frac{\partial^2}{\partial x^2} + \frac{\partial^2}{\partial y^2})\omega' \tag{6.98}$$

In view of Eqs. (6.95) and (6.96), we may assume that the vorticity perturbation has the form

$$\omega'(x,y,t) = \sum_{j=-\infty}^{\infty} \Omega_j\, e^{i(ukt - \mu_j x/\ell)} \tag{6.99}$$

Substituting Eq. (6.99) into Eq. (6.98), multiplying both sides of the equation by $\exp(i\mu_j x/\ell)$, and integrating over $0 < x < \ell$, one obtains

$$\frac{\partial^2}{\partial y^2}\Omega_j - [(\frac{\mu_j}{\ell})^2 + \frac{iuk}{\nu}]\Omega_j = 0 \tag{6.100}$$

Under the condition that the vorticity can diffuse only in the positive y-domain, the solution of Eq. (6.100) is found

to be

$$\Omega_j = \overline{\Omega}_j \exp\{-[(\frac{\mu_j}{\ell})^2 + \frac{iuk}{\nu}]^{\frac{1}{2}} y\}$$

Expanding the exponential function in a Taylor series about $y = 0$, and substituing the result into Eq. (6.99), we have

$$\omega'(x,y,t) = \sum_{j=-\infty}^{\infty} \overline{\Omega}_j \sum_{n=0}^{\infty} \frac{y^n}{n!} (-1)^n [(\frac{\mu_j}{\ell})^2 + \frac{iuk}{\nu}]^{\frac{n}{2}} e^{i(ukt - \mu_j x/\ell)} \tag{6.101}$$

However, from the definition of the vorticity, ω' also can be expressed as follows, using Eqs. (6.95) and (6.96),

$$\omega'(x,y,t) = \sum_{j=-\infty}^{\infty} \{uk(\frac{\mu_j}{\ell})H_j - A_{1j} - [(\frac{\mu_j}{\ell})^2 UH_j + 2A_{2j}]y + \text{higher order terms in } y\} e^{i(ukt - \mu_j x/\ell)} \tag{6.102}$$

Equating coefficients of y^n in Eqs. (6.101) and (6.102), one obtains

$$\overline{\Omega}_j = uk(\frac{\mu_j}{\ell})H_j - A_{1j} \tag{6.103}$$

$$\overline{\Omega}_j[(\frac{\mu_j}{\ell})^2 + \frac{iuk}{\nu}]^{\frac{1}{2}} = (\frac{\mu_j}{\ell})^2 UH_j + 2A_{2j} \tag{6.104}$$

Eliminating $\overline{\Omega}_j$ from these equations, we have

$$A_{1j} = uk(\frac{\mu_j}{\ell})H_j - [(\frac{\mu_j}{\ell})^2 + \frac{iuk}{\nu}]^{-\frac{1}{2}}[(\frac{\mu_j}{\ell})^2 UH_j + 2A_{2j}] \tag{6.105}$$

Now the Navier-Stokes equation for the perturbation velocities in the vicinity of the beam can be written as

$$\frac{\partial u'}{\partial t} + Uy \frac{\partial u'}{\partial x} + v'U = -\frac{1}{\rho_1} \frac{\partial p_1}{\partial x} + \nu \nabla^2 u' \tag{6.106}$$

Substituting Eqs. (6.66), (6.95) and (6.96) into Eq. (6.106) and letting $y = 0$, we obtain

$$\sum_{j=-\infty}^{\infty} [(i \frac{\mu_j}{\ell}) P_{1j} + \rho_1 \nu [U(\frac{\mu_j}{\ell})^2 H_j + 2A_{2j}]] \, e^{i(ukt - \mu_j x/\ell)}$$

$$= 0 \tag{6.107}$$

Multiplying both sides of the equation by $\exp(i\mu_j x/\ell)$ and integrating over $0 < x < \ell$, one obtains

$$A_{2j} = -\frac{1}{2\rho_1 \nu} \frac{i\mu_j}{\ell} P_{1j} - \frac{U}{2} (\frac{\mu_j}{\ell})^2 H_j \tag{6.108}$$

Substitution of Eq. (6.108) into Eq. (6.105) yields

$$A_{1j} = uk(\frac{\mu_j}{\ell}) H_j + \frac{1}{\rho_1 \nu} [(\frac{\mu_j}{\ell})^2 + \frac{iuk}{\nu}]^{-\frac{1}{2}} (\frac{i\mu_j}{\ell}) P_{1j} \tag{6.109}$$

Now, substituting Eqs. (6.108) and (6.109) into Eqs. (6.95) and (6.96), we have

$$u'(x,y,t) = \sum_{j=-\infty}^{\infty} R_j \, e^{i(ukt - \mu_j x/\ell)} \tag{6.110}$$

$$v'(x,y,t) = \sum_{j=-\infty}^{\infty} S_j \, e^{i(ukt - \mu_j x/\ell)} \tag{6.111}$$

where

$$R_j = -UH_j + \{uk(\frac{\mu_j}{\ell})H_j + \frac{1}{\rho_1 \nu}[(\frac{\mu_j}{\ell})^2 + \frac{iuk}{\nu}]^{-\frac{1}{2}}(\frac{i\mu_j}{\ell})P_{1j}\}y$$

$$+ \text{higher order terms in } y \qquad (6.112)$$

$$S_j = iukH_j - \frac{i\mu_j}{\ell} UH_j y + \text{higher order terms in } y \qquad (6.113)$$

We note that the velocity components, u' and v', obtained here are induced by a frozen-pattern component, $\exp[i(ukt - kx)]$, of the turbulent pressure p; therefore, $\sum_{j=-\infty}^{\infty} R_j \exp(-i\mu_j x/\ell)$ and $\sum_{j=-\infty}^{\infty} S_j \exp(-i\mu_j x/\ell)$ are the wave-number response functions of the velocity components, u' and v', respectively. Thus, the total velocities induced by the turbulent pressure p are obtained by superposition as follows:

$$u'(x,y,t) = \iint_{-\infty}^{\infty} \sum_{j=-\infty}^{\infty} R_j \, e^{i(ukt - \mu_j x/\ell)} \, dF(k,u) \, dG(u) \qquad (6.114)$$

$$v'(x,y,t) = \iint_{-\infty}^{\infty} \sum_{j=-\infty}^{\infty} S_j \, e^{i(ukt - \mu_j x/\ell)} \, dF(k,u) \, dG(u) \qquad (6.115)$$

The perturbation Reynolds stress near the beam can now be computed from

$$\tau(x,y) = \rho_1 E[u'v'] \qquad (6.116)$$

Substituting Eqs. (6.112)-(6.115) into Eq. (6.116), one obtains

$$\tau(x,y) = \int_{-\infty}^{\infty}\int \sum_{n=-\infty}^{\infty} \sum_{j=-\infty}^{\infty} T_{nj}(k,u,y)\, e^{i2\pi(j-n)x/\ell}$$

$$S_p(k,u)\, dk\, du \qquad (6.117)$$

where

$$T_{nj}(k,u,y) = \rho_1 R_n S_j^* \qquad (6.118)$$

As in the preceding section, the integration variable u in Eq. (6.117) may be replaced by ω/k and the wave-number spectrum of the turbulence pressure, S_p, replaced by the frequency spectrum to give

$$\tau(x,y) = \int_{-\infty}^{\infty}\int \sum_{n=-\infty}^{\infty} \sum_{j=-\infty}^{\infty} T_{nj}(k,\frac{\omega}{k},y)\, e^{i2\pi(j-n)x/\ell}$$

$$\bar{\Phi}_p(0,\omega)\, \Psi(k - \frac{\omega}{U_c})\, dk\, d\omega \qquad (6.119)$$

where the specific expression for T_{nj}, obtained by substituting Eqs. (6.112) and (6.113) into Eq. (6.118) is given as follows:

$$T_{nj}(k,\frac{\omega}{k},y) = \rho_1 i\omega U H_n H_j^* + \rho_1 \{-i(\frac{\mu_j}{\ell})U^2 H_n H_j^*$$

$$- i\omega^2(\frac{\mu_n}{\ell})H_n H_j^* + \frac{1}{\rho_1 \nu}\omega(\frac{\mu_n}{\ell})[(\frac{\mu_n}{\ell})^2 + \frac{i\omega}{\nu}]^{-\frac{1}{2}} P_{1n} H_j^*\}\, y$$

$$+ \text{higher order terms in } y \qquad (6.120)$$

Since the structural motion is a stationary random process in time, the first term in the expression of T_{nj} does not contribute to the integral when substituted into Eq. (6.119). In this periodic beam case, however, the spatial homogeneity of

the structural motion is destroyed because of the supports. Consequently, the perturbation Reynolds stress near a periodic beam is a function of the spatial variable x. A reasonable measure of the net effect of the perturbation Reynolds stress appears to be the spatial average defined as follows:

$$\langle \tau(y) \rangle = \frac{1}{\ell} \int_0^{\ell} \tau(x,y)\, dx \tag{6.121}$$

Again, define a Reynolds number

$$R = \frac{\omega \ell^2}{\nu \mu_n^2} \tag{6.122}$$

Eqs. (6.119) and (6.120) may be substituted into Eq. (6.121), and the result is simplified by expanding the square-root term in a Taylor series about $1/R = 0$. Keeping only the real part of the expression which represents the physical average Reynolds stress, one obtains

$$\langle \tau(y) \rangle = \int_{-\infty}^{\infty} \sum_{n=-\infty}^{\infty} \frac{\omega}{\sqrt{2\nu|\omega|}} \left(\frac{\mu_n}{\ell}\right) P_{1n}(k, \tfrac{\omega}{k}, 0)\, H_n^*(k, \tfrac{\omega}{k})\, y \, \bar{\Phi}_p(0,\omega)\, \Psi(k - \tfrac{\omega}{U_c})\, dk\, d\omega \tag{6.123}$$

Finally, substitution of Eqs. (6.67) into Eq. (6.122) yields

$$\langle \tau(y) \rangle = \int_{-\infty}^{\infty} \sum_{n=-\infty}^{\infty} \frac{\rho_1 \omega}{\sqrt{2\nu|\omega|}} \left(\frac{\mu_n}{\ell}\right)^2 \left(\frac{\omega \ell}{\mu_n} - U_\infty\right)^2 |H_n|^2\, y \, \bar{\Phi}_p(0,\omega)\, \Psi(k - \tfrac{\omega}{U_c})\, dk\, d\omega \tag{6.124}$$

6.4 Concluding Remarks

Expressions for the perturbation Reynolds stress induced by fluid-solid interaction were obtained for two structural models. The first structural model, an infinite unsupported beam, was used to develope the basic concepts of the analysis. The results were then extended to the second model of an infinite beam, simply-supported at equal intervals. The second model is a more realistic model for the typical fuselage construction of an airplane. The effect of the radiation pressure was included in the formulation. The perturbation Reynolds stress involves a double integration with an integrand depending on the beam motion and radiated pressure. The complexity of the expression permits only qualitative discussions in this thesis. Hopefully, quantitative results can be documented after extensive numerical studies in the future.

The radiation pressure, p_1, required in the present analysis has been obtained from a wave equation for inviscid fluid. More rigorously the viscosity in the fluid and the velocity profile in the boundary layer should be taken into account when determining the radiation pressure. However, at the present time no closed form solution is known of this more accurate wave equation.

VII. GENERAL CONCLUSION

This investigation has been concerned with the interaction between a turbulent flow and certain types of structure responding to its excitation. The turbulence is typical of those associated with a boundary layer, having a cross-spectral density indicative of convection and statistical decay. It has been shown that a decaying turbulence can be constructed from superposing infinitely many components, each of which is convecting as a frozen-pattern at a different velocity. This turbulence decomposition scheme reduces greatly the computation time by reducing to one-half the number of integration which must be performed on a computer. Furthermore, the scheme provides a convenient way in which experimentally measured cross-spectral density of the turbulent pressure fluctuation can be incorporated directly into the computation.

The results of the structure-turbulence interaction were presented in terms of the spectral densities of the structural response and the perturbation Reynolds stress in the fluid at the vicinity of the interface. A number of structural models were considered in the investigation. Among the one-dimensional models were an unsupported infinite beam and a periodically supported infinite beam. The first model was used to develope the basic ideas which were then applied to the more realistic second model resembling the fuselage construction of an aircraft. For the two-dimensional case a simple membrane was used to illustrate the type of

formulation applicable to most two-dimensional structures. However, a small random variation in the membrane tension was included in the analysis since ideally uniform tension never exists in practice. Moreover, the mathematical approach used in dealing with random membrane tension can be adapted to treat other random structural properties in general. Both the one-dimensional and two-dimensional structures mentioned above were backed by a space filled with an initially quiescent fluid to simulate the acoustic environment when the structure forms one side of a cabin of a sea- or aircraft.

It has been found that important spectral peaks of the structural response will not appear if decays in the turbulence is neglected in the analysis. Thus, the usual Taylor's hypothesis of frozen-pattern turbulence is unconservative as far as the assessment of structural reliability is concerned. The perturbation Reynolds stress is indicative of the change in the skin-friction drag due to structural motion. It has been shown that, given the statistical information of the boundary-layer turbulent pressure field, the perturbation Reynolds stress can be altered by varying the structural parameters. Therefore, the present study is potentially useful for designing flight or marine structures to minimize the total skin-friction drag.

REFERENCES

1. Ribner, H.S., "Boundary-Layer-Induced Noise in the Interior of Aircraft", UTIA Report No. 37, April 1956.

2. Corcos, G.M., and Liepmann, H.W., "On the Contribution of Turbulent Boundary Layers to the Noise Inside a Fuselage", NACA TM-1420, September 1956.

3. Pretlove, A.J., "Free Vibrations of a Rectangular Panel Backed by a Closed Rectangular Cavity", J. of Sound and Vibration, 2(3), 1965, pp. 197-209.

4. Pretlove, A.J., "Forced Vibrations of a Rectangular Panel Backed by a Closed Rectangular Cavity", J. of Sound and Vibration, 3(3), 1966, pp. 252-261.

5. Dowell, E.H., "Transmission of Noise from a Turbulent Boundary Layer through a Flexible Plate into a Closed Cavity", J. of Acoustical Society of America, Vol. 46, No. 1(Part 2), 1969, pp. 238-252.

6. Chyu, W.J., and Au-Yang, M.K., "Response of Panels to Turbulence-Induced, Surface Pressure Fluctuations and Resulting Acoustic Radiation to the Flowfield", Paper 73-993, AIAA Aero-Acoustics Conference, Seattle, Washington, October 15-17, 1973.

7. Yen, D.H.Y., Maestrello, L., and Padula, S., "On an Integro-Differential Equation Model for the Study of the Response of an Acoustically Coupled Panel", AIAA Second Aeroacoustics Specialists Conference, Hampton, Virginia, March 24-26, 1975.

8. Leibowitz, R.C., "Vibratory Response and Acoustical Radiation of a Water-Loaded Turbulence-Excited Plate-Cavity System-Option 6", Ship Acoustics Department Research and Development Report, July 1975, Report 2976F.

9. Leibowitz, R.C., "Vibroacoustic Response of Turbulence Excited Thin Rectangular Finite Plates in Heavy and Light Fluid Media", J. of Sound and Vibration, 40(4), 1975, pp. 441-495.

10. Pestel, E.C., and Leckie, F.A., "Matrix Methods in Elastomechanics", McGraw-Hill Book Company, New York, 1963.

11. Lin, Y.K., and Donaldson, B.K., "A Brief Survey of Transfer Matrix Techniques with Special Reference to the Analysis of Aircraft Panels", J. of Sound and Vibration, 10(1), 1969, pp. 103-143.

12. Lin, Y.K., Brown, I.D., and Deutschle, P.C., "Free Vibration of a Finite Row of Continuous Skin-Stringer Panels", J. of Sound and Vibration, I, 1964, pp. 14-27.

13. Lin, Y.K., and McDaniel, T.J., "Dynamics of Beam-Type Periodic Structures", J. of Engineering for Industry, November 1969, pp. 1133-1141.

14. Vaicaitis, R., and Lin, Y.K., "Response of Finite Periodic Beam to Turbulent Boundary-Layer Pressure Excitation", AIAA Journal, Vol. 10, No. 8, August 1972, pp. 1020-1024.

15. Vaicaitis, R., Doi, K., and Lin, Y.K., "Spatial Decay in the Response of Damped Periodic Beam", J. of Aircraft, Vol. 9, No. 1, January 1972, pp. 91-93.

16. Maekawa, S., "Structural Response of Multispan Panels in Turbulence and Acoustic Environment", M.S. Thesis, University of Illinois at Urbana-Champaign, 1975.

17. Brillouin, L., "Wave Propagation in Periodic Structures", Dover Publications, New York, 1953.

18. Mead, D.J., "Vibration Response and Wave Propagation in Periodic Structures", Journal of Engineering for Industry, Transaction ASME, Vol. 93(B), 1971, pp. 783-792.

19. Mead, D.J., and Pujara, K.K., "Space-Harmonic Analysis of Periodically Supported Beams: Response to Convected Random Loading", J. of Sound and Vibration, 14(4), 1971, pp. 525-541.

20. Sen Gupta, G., "Dynamics of Periodically Stiffened Structures using a Wave Approach", AFML-71-99, Air Force Materials Laboratory, Ohio, May 1971.

21. Orris, R.M., and Petyt, M., "Random Response of Periodic Structures by a Finite Element Technique", J. of Sound and Vibration, 43(1), 1975, pp. 1-8.

22. Sen Gupta, G., "On the Relation between the Propagation Constant and the Transfer Matrix used in the Analysis of Periodically Stiffened Structures", Letters to the Editor, J. of Sound and Vibration, 11(4), 1970, pp. 483-484.

23. Corcos, G.M., "Resolution of Pressure in Turbulence", J. of Acoustical Society of America, Vol. 35, No. 2, February 1963, pp. 192-199.

24. Bull, M.K., "Properties of the Fluctuating Wall-Pressure Field of a Turbulent Boundary Layer", University of Southampton Report, A.A.S.U. 234, March 1963 (Also AGARD Rep. No. 455, 1963).

25. Willmarth, W.W., and Wooldridge, C.E., "Measurements of the Fluctuating Pressure at the Wall Beneath a Thick Turbulent Boundary Layer", University of Michigan Report 02920-1-T, April 1962 (Also J. Fluid Mechanics, Vol. 14, 1962, p. 187).

26. Maestrello, L., "Measurements and Analysis of the Response Field of Turbulent Boundary Layer Excited Panels", J. of Sound and Vibration, 2(3), 1965, pp. 270-292.

27. Maestrello, L., "Design Criterion for Minimum Structural Response and Sound Radiation of a Panel Excited by a Turbulent Boundary Layer", AIAA 5th Aerospace Sciences Meeting, New York, New York, January 23-26, 1967.

28. Maestrello, L., Mouteith, J.H., Manning, J.C., and Smith, D.L., "Measured Response of a Complex Structure to Supersonic Turbulent Boundary Layers", AIAA 14th Aerospace Sciences Meeting, Washington D.C., January 26-28, 1976.

29. Lin, Y.K., and Maekawa, S., "A New Look at Decomposition of Turbulence Forcing Field and the Structural Response", to be published in AIAA Journal.

30. Lin, Y.K., Maekawa, S., Nijim, H.H., and Maestrello, L., "Response of Periodic Beam to Supersonic Boundary-Layer Pressure Fluctuations", IUTAM Symposium on Stochastic Problems in Dynamics, University of Southampton, England, July 19-23, 1976.

31 Morse, P.M., and Ingard, K.U., "Theoretical Acoustics", McGraw-Hill Book Company, New York, 1968.

32. Richards, E.J., and Mead, D.J., "Noise and Acoustic Fatigue in Aeronautics", John Wiley and Sons Ltd., London, 1968.

33. Lin, Y.K., and Yang, J.N., "Free Vibration of a Disordered Periodic Beam", J. of Applied Mechanics, 41, 1974, pp. 383-391.

34. Yang, J.N., and Lin, Y.K., "Frequency Response Functions of a Disordered Periodic Beam", J. of Sound and Vibration, 38, 1975.

35. Lin, Y.K., "Mechanics Today, Chapter III; Random Vibration of Periodic and Almost Periodic Structures", ed. S. Nemat-Nasser, Pergamon Press, 1976.

36. Blick, E.F., Bert, C.W., Reed, T.D., Walters, R.W., and Wares, R.N., "Aerodynamic Drag Reduction Using Compliant Coatings", Proceedings of The Oklahoma Academy of Science for 1966.

37. Fischer, M.C., Weinstein, L.M., Ash, R.L., and Bushnell, D.M., "Compliant Wall-Turbulent Skin-Friction Reduction Research", AIAA Eighth Fluid and Plasma Dynamics Conference, Hartford, Connecticut, June 16-18, 1975.

38. Ljatkher, V.M., "Hydrodynamic Effect of Turbulent Flow on Flow Boundaries", IUTAM-IAHR, Flow-Induced Structural Vibrations Symposium, Karlsruhe, Germany, August 14-16, 1972.

39. Black, T.J., "Viscous Drag Reduction Examined in the Light of a New Model of Wall Turbulence", Proceedings of the Symposium on Viscous Drag Reduction, Dallas, Texas, September 24-25, 1968.

40. Black, T.J., "An Analytical Study of the Measured Wall Pressure Field under Supersonic Turbulent Boundary Layers", NASA CR-888, April 1968.

41. Blick, E.F., "The Theory of Skin Friction Reduction by a Compliant Coating in a Turbulent Boundary Layer", Proceedings of the Symposium on Viscous Drag Reduction, Dallas, Texas, September 24-25, 1968.

42. Schlichting, H., "Boundary-Layer Theory", translated by J. Kestin, McGraw-Hill Book Company, New York, 1968.

43. Lin, Y.K., "Probabilistic Theory of Structural Dynamics", McGraw-Hill Book Company, New York, 1967.

44. Monin, A.S., and Yaglom, A.M., "Statistical Fluid Mechanics: Mechanics of Turbulence", MIT Press, Cambridge, Massachusetts, 1971.

45. Selby, S.M., "Standard Mathematical Tables", 21st. ed., The Chemical Rubber Co., Cleveland, Ohio, 1973.

46. Abramowitz, M., and Stegun, I.A., "Handbook of Mathematical Functions", AMS 55, 1964.

47. Timoshenko, S., and Young, D.H., "Vibration Problems in Engineering", D. Van Nostrand Co., New York, 1955.

48. Ffowcs Williams, J.E., "Reynolds Stress Near a Flexible Surface Responding to Unsteady Air Flow", Bolt Beranek and Newman Inc., Report No. 1138, June 1964.

NASA-Langley, 1977